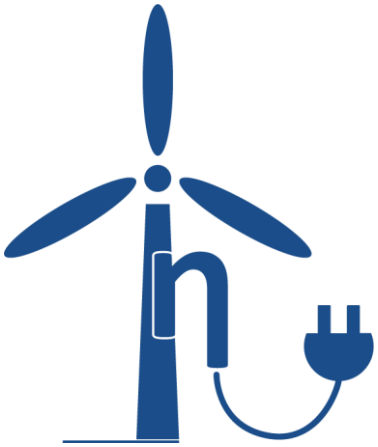

Deliverable D3 within 19ENG08

- Report describing the calibration of the 5 MN m torque transfer standard partially up to 1.1 MN m with an uncertainty < 0.1 % and in the full range up to 5 MN m with an uncertainty < 0.5 % with synchronised measurements of rotational speed up to 20 min^{-1} on the low-speed shaft respectively torque measurements up to 100 kN m with synchronised measurements of rotational speed up to 1600 min^{-1} on the high-speed shaft -

Authors: Paula Weidinger (PTB), 2023

Zihang Song (PTB)

Rafael Soares de Oliveira (Inmetro)

Lukáš Vavrečka (CMI)

Janusz Fidelus (GUM)

Timo Kananen (VTT)

Marcel Heller (FhG)
Hongkun Zhang (FhG)

DOI: 10.5281/zenodo.8112428

This report has been produced within the EMPIR project entitled *Traceable Mechanical and Electrical Power Measurement for Efficiency Determination of Wind Turbines* or *19ENG08 WindEFCY.* More information about this collaborative research project can be found on the project's website https://www.ptb.de/empir2020/windefcy/home/. This report describes the calibration of the 5 MN m torque transfer standard partially up to 1.1 MN m including an extrapolation of the calibration results up to 5 MN m as well as the use of the transducer under rotation up to 22.5 rpm. Moreover, a 125 kN m torque transducer was calibrated statically for usage under rotation up to 1600 rpm. Other influences on statically calibrated transducers when used in test benches, such as different data acquisition and filter settings, rotational speed and non-step application of loads, were investigated.

Disclaimer

Any mention of commercial products within this report is for information only; it does not imply recommendation or endorsement by the partners in this project.

The views expressed in this report are those of the authors and of the EMPIR 19ENG08 WindEFCY project team.

Acknowledgement of funding

The production of this project and, therefore, this report was funded by the European Metrology Programme for Innovation and Research (EMPIR). The EMPIR initiative is co-funded by the European Union's Horizon 2020 research and innovation programme and the EMPIR Participating States.

Authorship

The preparation of this guide was led by Paula Weidinger of the Physikalisch-Technische Bundesanstalt (PTB), Braunschweig (Germany) with extensive input from all members of the EMPIR 19ENG08 project team. The discussion and input of all the partners in the project and their colleagues are greatly appreciated.

Suggestion for the quotation of the references

P Weidinger *et al*, 2023. Deliverable D3 within 19ENG08: Report describing the calibration of the 5 MN m torque transfer standard. DOI: 10.5281/zenodo.8112428

Project logo

DOI: 10.5281/zenodo.7043161

Content

DOI: 10.5281/zenodo.8112428

DOI: 10.5281/zenodo.8112428

1 Introduction

In recent years, the utilisation of renewable energy sources has gained significant attention due to the increasing concerns about climate change and the depletion of fossil fuels. Amont the various renewable energy options, wind energy has emerged as one of the most promising and rapidly growing sources of clean power. Wind turbines are capable of harnessing the kinetic energy of wind and converting it into electricity, providing an environmentally friendly alternative to conventional power generation methods.

The efficient operation and performance optimisation of wind turbines are of paramount importance for maximising their power output and ensuring their long-term viability. Accurate prediction of wind energy performance and precise measurement of torque in the wind energy sector play a crucial role in achieving these objectives.

Precise torque measurement is not only important in test benches for wind turbines on the low-speed shaft (LSS) with rotational speed up to 20 min^{-1}, but also in wind turbines themselves, the torque under rotation should be measured as precisely as possible on the high-speed shaft (HSS). For a reliable torque measurement, a traceability to national standards by means of calibration is necessary. A transfer standard with a measuring capacity of 5 MN m was specially established for torque calibration under rotation on the LSS. The partial range calibration up to 1.1 MN m and an extrapolation of the calibration results up to 5 MN m as well as the use of the transducer under rotation up to 22.5 min^{-1} is described in chapter 3.

A torque transducer with a nominal measuring range of 125 kN m was calibrated for a traceable torque measurement on the HSS. Since a calibration under rotation is currently not possible worldwide, various analyses regarding the influence of rotation up to 1300 min^{-1} on the torque measurement were investigated using theoretical calculations (section 2.4), statically calibrated transducers (section 3.1) and different data acquisition and filtering (chapter 5). All used transducers are calibrated to national standards units using standard calibration procedures to evaluate their performance and deviation from the national standard in a static, step-by-step manner as described in chapter 2.

Moreover, as in reality torque load due to wind power is unpredictable and does not follow given sequences as in standard calibration procedure, two different load configurations to test the transducer response to non-traditional calibration loads were developed and examined. The approaches and results are described in chapter 4.

This report was generated in Work Package 2 (WP2) of the EMPIR project 19ENG08 “Traceable mechanical and electrical power measurement for efficiency determination of wind turbines” short WindEFCY.

DOI: 10.5281/zenodo.8112428

2 Calibration of torque transducers – state of the art

Torque transducers convert torque into an electrical signal. Especially for static torque measurement, strain gauges (SGs) are used for the signal conversion thanks to their good linearity and reproducibility, high precision, and small hysteresis. However, foil SGs are also suitable for dynamic torque measurements with high frequencies up to 10 000 m/s² and even centrifugal accelerations due to their low weight. For a wider use of torque transducers with SGs in different fields, temperature effects on SGs can be compensated. With this measuring principle, torques can also be measured in the positive and negative directions. [1]

Torque measurement with SGs is an indirect torque conversion: the mechanical deformation of the spring or deformation body is transferred to the SGs glued to it, which also deforms them, changing the conductor resistance and ultimately the output signal. Usually, four SGs are interconnected in a Wheatstone bridge configuration to be able to measure the very small ohmic resistance changes, which in turn can then be amplified. More information about SGs and their application can be found in [2].

To trace the torque measurement with SGs to national standard units, standard calibration procedures using torque standard machines (TSMs) are used. In a standard calibration procedure, the transducer's performance and its deviation from the national standard is evaluated. So far, these type of calibration is done statically and in a stepwise manner. Besides the existing body types of torque transducers, different TSMs, which where all used for further analyses in this report, and a typical static torque calibration procedure are described in the following.

2.1 Existing body types of torque transducers

The shape of the spring body that undergoes linear-elastic deformation when subjected to torque can be varied. Figure 1 shows commonly used designs, such as a solid (a), hollow shaft or flange (b), and square-section shaft (d) types, where torsional stress is sensed by the SGs. Hollow shafts provide higher bending stiffness for the same load-bearing profile area, while solid square-section shafts are used for high torque ranges. In spoked wheel (e) and cage shaped (f, g) transducers, local flexural stress in sub-elements is generated. These transducers are suitable for low torques due to the high strain values resulting from their design. Another torque measurement option is the shear principle invented by HBK (Hottinger, Brüel & Kjær), which uses beams as shear elements with SGs applied to them. These shear transducers have excellent lateral stiffness perpendicular to the measurement direction. [1]

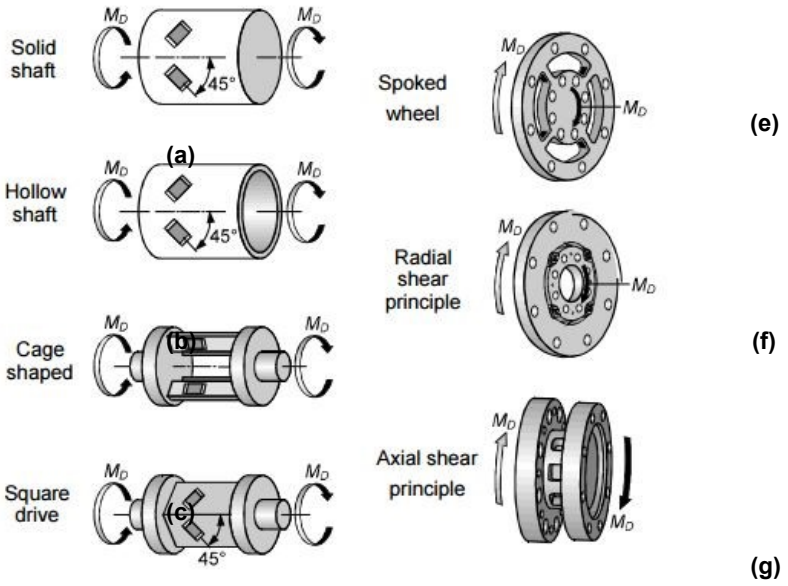

Figure 1: Different shapes of torque transducer deformation bodies, taken from [1]**.**

DOI: 10.5281/zenodo.8112428

There is also a variety of shapes for the connections between the deformation body and the rest of the system, which is also shown in Figure 1. However, the square-drive plug-in connection is not included in the figure. Although this type of connection is easy to use, it has a significant drawback of producing backlash between the adapters when torque is applied. To eliminate the backlash, mechanical or hydraulic clamping connections are used for low torque up to a few kN m. For higher torque ranges, bolted flanges are a practical option. [1]

2.2 Torque standard machines

Various TSMs at different national metrology institutes (NMIs) were used for the different measurements. In the following the 2 kN m, the 5 kN m and the 1.1 MN m and the 5 MN m reference TSMs at the VTT, at the GUM and at the PTB are presented, as well as the 1 kN m and the 20 kN m direct loading machines at the CMI and at the PTB.

2.2.1 1 kN m dead-weight torque standard machine at CMI

The TSM at CMI (Figure 2), Czech Metrology Institute, is a dead-weight TSM, where the torque magnitude is generated by dead weights suspended on a lever-arm in the gravitational field of the earth.

The TSM has two weight systems. One system is for the realisation of clockwise torque and the second system is for the realisation of anti-clockwise torque. Each system contains 19 bodies made of stainless austenitic steel for generated torque in the range from 2 N m up to 1 kN m. The lever-arm is double reversible with the same length for each torque direction. At the time of the measurement, the lever-arm was mounted in a pair of ball bearings.

Between 2017 and 2021, as part of the National Metrology System (NMS) development concept, the TSM was converted to using an air bearing. This conversion allowed the expanded relative measurement uncertainty (MU) to be reduced from 0.05 % to 0.01 % (k = 2).

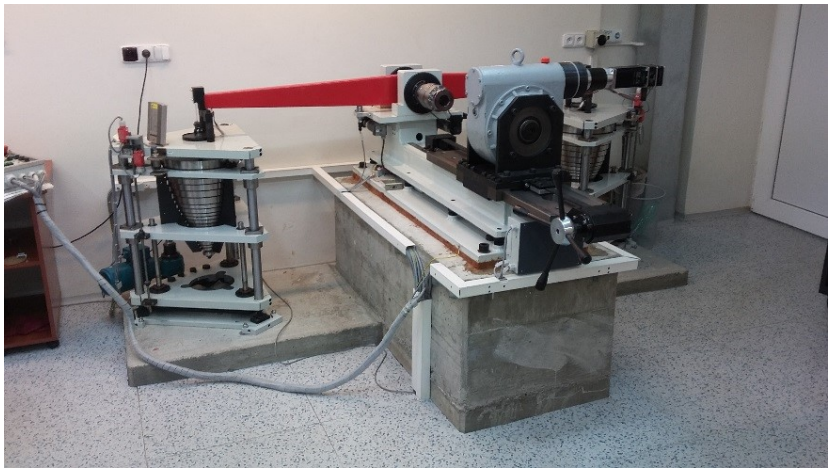

Figure 2: CMI's 1 kN m dead-weight TSM.

2.2.2 2 kN m dead-weight torque standard machine at VTT

VTT, the Technical Research Center of Finland, owns a 2 kN m dead-weight TSM (Figure 3) with a measuring capacity from 4 N m up to 2 kN m. The expanded relative MU in the range 4 N m to 200 N m is 8×10^{-4} (k = 2). In the range from 20 N m to 2000 N m, the expanded relative MU is 5×10^{-4} (k = 2). These values apply to clockwise and anti-clockwise torque respectively. The read out unit is a DMP40 amplifier.

This machine was used for the analyses in chapter 4. For these analyses it is important to know that the mass loading of this 2 kN m dead-weight TSM is comparatively slow. Loading from 0 % up to 100 % takes about 1 min, partial loading can be achieved in about 30 s (15 s for loading and another 15 s for the stabilisation).

DOI: 10.5281/zenodo.8112428

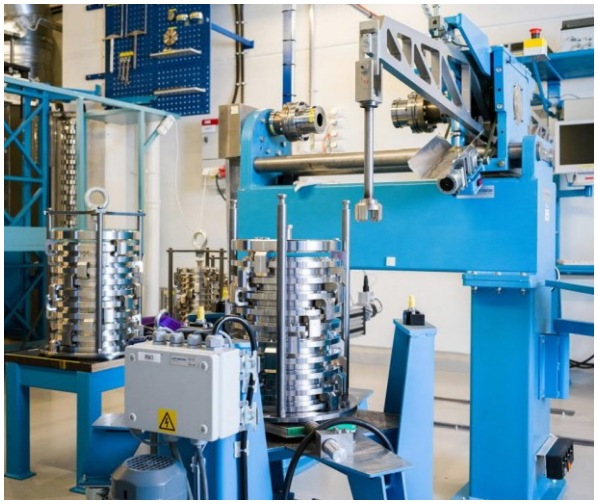

Figure 3: VTT's 2 kN m dead-weight TSM.

2.2.3 5 kN m reference torque standard machine at GUM

The TSM at GUM (Figure 4), Central Office of Measures in Poland, is a reference machine using a DC motor to apply torque and a calibrated reference torque transducer to measure torque. It is able to generate clockwise and anti-clockwise torque in a range from 10 N m up to 5 kN m with an expanded relative MU of 0.04 % (k = 2). The amplifiers deployed are a DMP 40 S2 and an MGCplus with an ML38 measuring card (resolution of 0.000001 mV/V, filter 0.5 Hz Bessel, ± 2.5 mV/V) both manufactured by HBK.

The reference transducers (HBK) in GUM's TCM realise the following measuring ranges:

- from 10 N m to 200 N m (type TB2 / 100 N m, #173530074)
- from 50 N m to 1000 N m (type TB2 / 500 N m, #182730038)
- from 200 N m to 5000 N m (type TB2 / 3000 N m, #181030110)

They can be used for clockwise and anti-clockwise torque applications with a calibration range from 10 N m to 5 kN m.

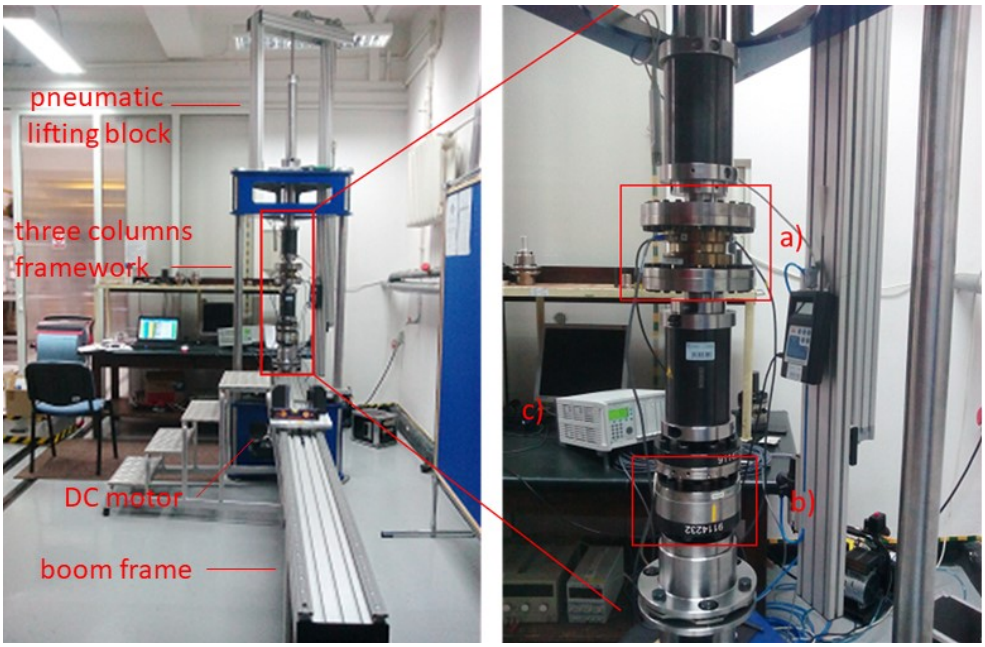

Figure 4: GUM's 5 kN m reference TSM: a) PTB's 2 kN m torque transducer (upper part), b) GUM's 3 kN m torque transducer (lower part), c) MGCplus / ML38 measuring amplifier.

DOI: 10.5281/zenodo.8112428

Creep study

A creep study was carried out for the 2 kN m torque transducer (in clockwise and anti-clockwise directions) on GUM's 5 kN m reference TSM (Figure 4). The tests were performed according to ISO 376:2011 standard [3].

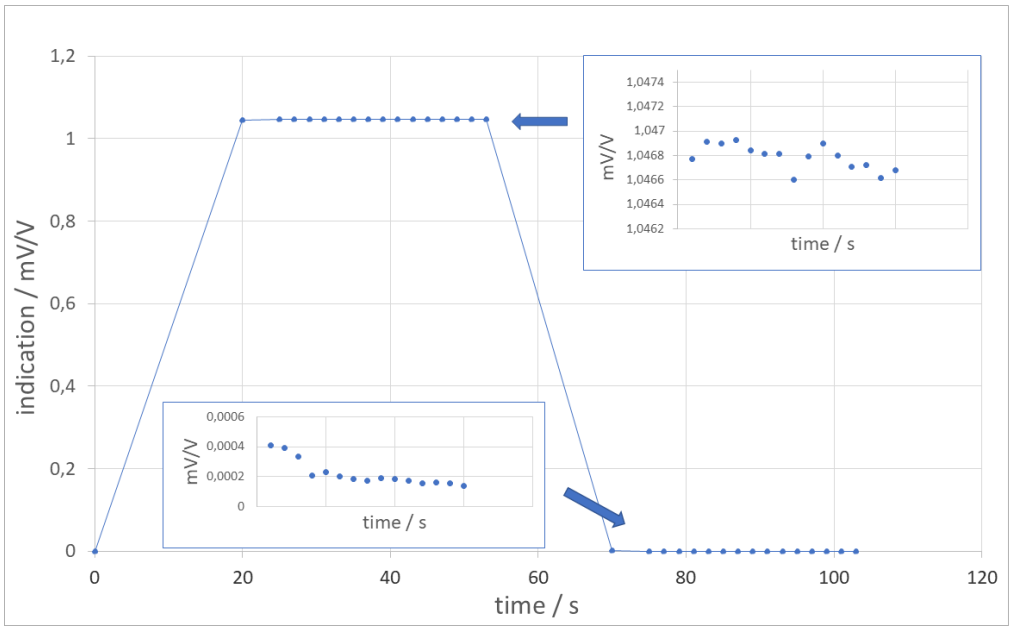

Figure 5: Graph of the 2 kN m torque transducer indication given in electrical units (mV/V) versus time (s) for measurements carried out after applying the maximum reference torque (at 2 kN m, ~ 1.04 mV/V) and for measurements conducted after removing the maximum reference torque. The insets represent the creep in the first 30 s of the measurement after the load application. For clarity, there are no error bars [4]**.**

The investigations were done for eight measurement points from 200 N m to 2000 N m. The creep of the 2 kN m torque transducer for measurements after applying the maximum reference torque of 2 kN m and for measurements after removing this reference torque is shown in Figure 5. The mV/V reading was measured after 5 s and then every 2 s for the first 30 s after the desired torque was applied or released. After applying the maximum reference torque of 2 kN m, the creep was minimal; a plateau can be observed (Figure 5, upper inset). On the other hand, removing the maximum reference torque (after applying M_{max} for 35 s) showed an increase in creep in the first few seconds (Figure 5, lower inset) [4]. A detailed creep analysis is included in another work prepared by GUM and PTB.

2.2.4 20 kN m dead-weight torque standard machine at PTB

The PTB conducted measurements using a dead-weight TSM (Figure 6) that has a horizontal measuring axis and a calibration capacity of 100 N m up to 20 kN m. The torque is created using weight stacks in a known gravitational field, which act as a force at a distance relative to the fixed fulcrum. The TSM reduces parasitic forces and bending moments by using thin metal foil instead of joints to attach the mass stacks to the lever arm, and multiple-plate clutches to diminish parasitic influences at the mechanical adapters of the torque transducer being calibrated. The double-sided lever arm allows for both clockwise and anti-clockwise torque application. Air bearings support the lever arm to minimise friction at the centre of rotation and lateral forces on the torque transducer. A counter drive maintains the horizontal position of the lever arm and ensures thereby a constant lever arm length during calibration. The TSM has an expanded relative MU of $2 \cdot 10^{-5}$ ($k = 2$) due to its unique design. [5]

DOI: 10.5281/zenodo.8112428

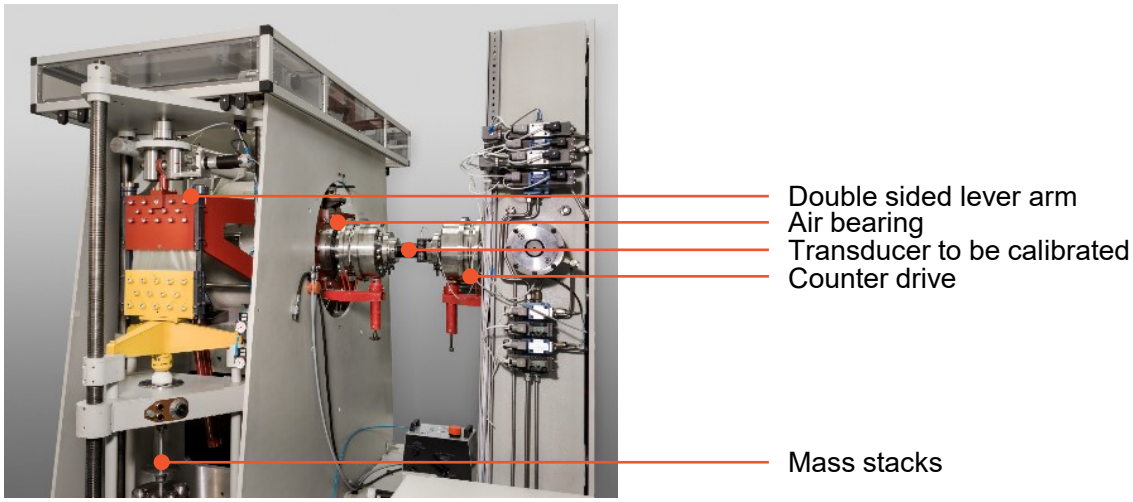

Figure 6: PBT's 20 kN·m dead-weight TSM, adapted from [5]**.**

2.2.5 1.1 MN m reference torque standard machine at PTB

The PTB in Braunschweig, Germany, has been capable of calibrating torque measurements up to 1.1 MN m since 2004, making it the world's largest torque calibration machine until 2023. This machine, illustrated in Figure 7, has a vertical measuring axis and is composed of a drive unit at the bottom, an additional reference torque transducer located below the transducer being calibrated, and a measuring arm with force transducers at the top. The machine utilises two servo-electric spindles at the bottom to apply torque by driving a double-sided lever arm in a free-floating manner, in the same direction and parallel to each other. The measuring arm at the top is also double-sided and divides the torque into two equal forces, which are measured using two force transducers. Each force transducer is connected to the measuring arm via a multi-component strain-controlled hinge, and the strain gauge bridges of these hinges measure the parasitic bending moments and transverse forces, which are minimised. This machine serves as a national standard with an expanded MU of 0.08 % (k = 2) within the measurement range of 100 kN m to 1100 kN m. [6]

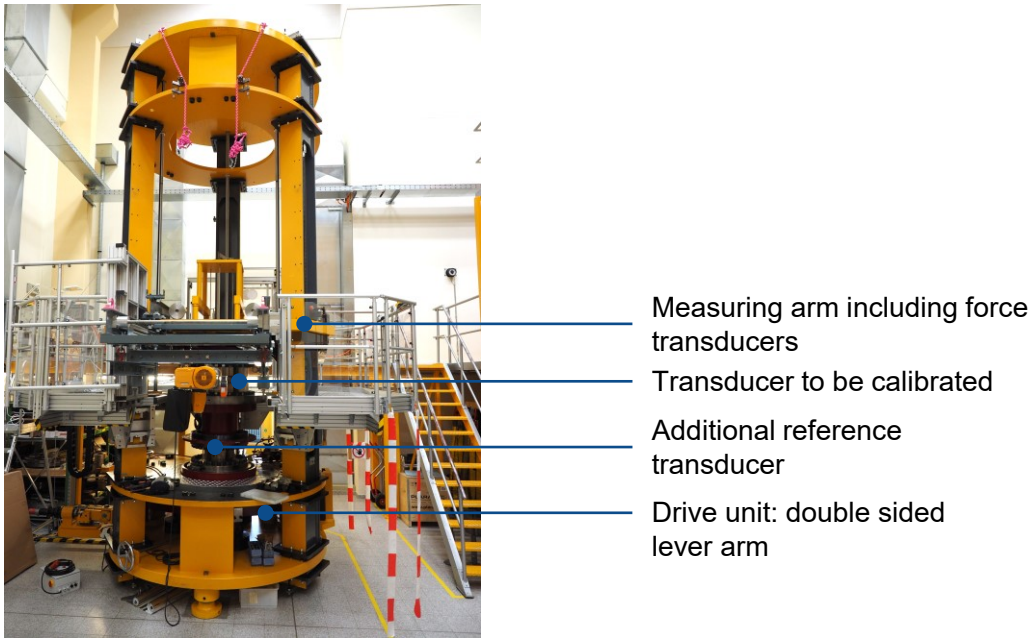

Figure 7: 1.1 MN·m reference TSM at the PTB.

2.2.6 5 MN m reference torque standard machine at PTB

The world's largest torque standard machine with a nominal measuring range of 5 MN m will soon be put into operation at the PTB. Other than PTB's 1.1 MN m, the measuring axis of the new 5 MN m is horizontal. Figure 8 displays the final design of the 5 MN m reference TSM. The machine operates within this 5 MN m range using two 1.2 MN cylinders to generate torque and four 100 kN cylinders to produce bending moments and axial forces. The anticipated relative expanded MU for the 5 MN m torque range is < 0.5 % (k = 2). [7]

The reference TSM is not only capable of producing torque but also bending moments and axial and shear forces, which can be combined as required with the capacity of the hydraulic cylinders. The forces and moments are generated through servo-hydraulic cylinders mounted on the machine's actuator lever arm. The resulting torque is then transferred through the device under test (DUT) to the measuring lever. The foundation on which the machine is mounted is responsible for absorbing the reaction forces initiated by the torque excitation and regulating the position and level of the machine. The measuring side is rigidly connected to the foundation, while the actuator side can be shifted using a linear guide unit, allowing for adjustment of the mounting space for the DUT as required. [7]

The measuring side of the TSM includes a reference measuring system that consists of force transducer and a measuring lever. Flexure hinges are used to decouple force and moment shunts, reducing systematic errors. The measuring strings are adjusted to have maximum stiffness for torque and minimum stiffness for other degrees of freedom. The torque is measured using two vertical torque measuring strings and the bending moments and axial force are measured through four horizontal measuring strings. The reference torque is calculated by factoring in the shear force shunts and angles between the measuring strings and the lever. The force transducers are calibrated in PTB's 2 MN dead-weight force standard machine with a relative uncertainty of $2 \cdot 10^{-5}$ (k = 2). [7]

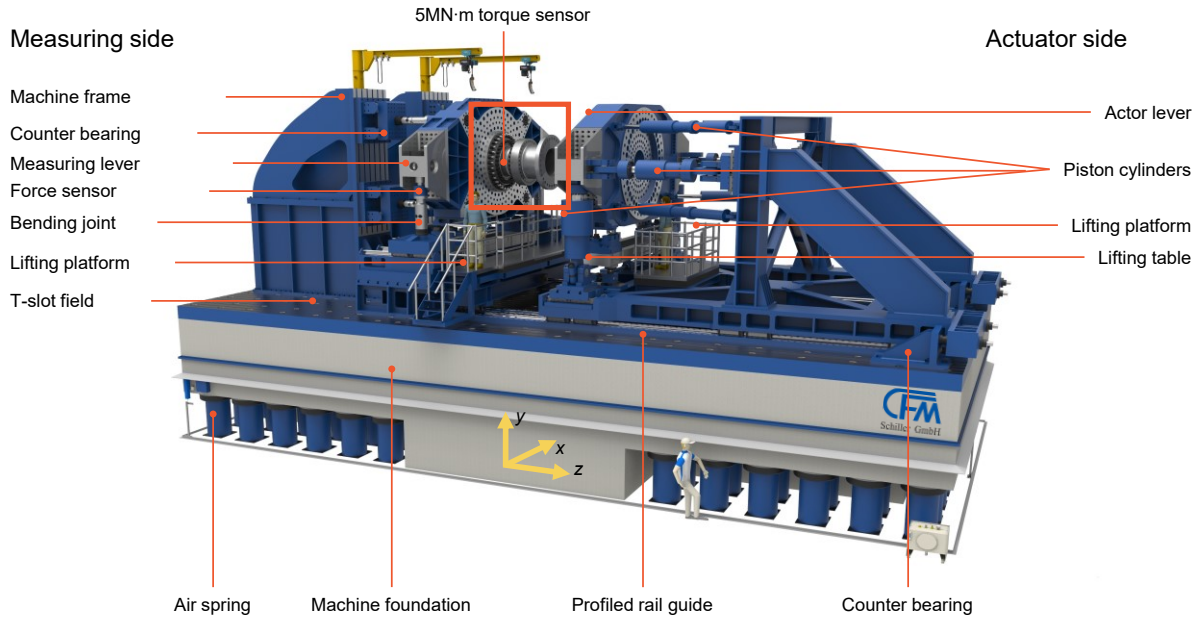

Figure 8: 5 MN m reference TSM at the PTB, based on [7]**.**

2.3 Static calibration procedure acc. to DIN 51309 / Euramet cg-14

Different methods are used in NMIs to realise torque, which include dead-weight TSMs, force-lever TSMs, and reference TSMs. All calibrations are carried out using specific procedures that are described in guidelines such as EURAMET calibration guide cg-14 [8] or DIN 51309 [9]. Both guidelines stipulate certain conditions and procedures that must be followed during calibration, and as they are quite similar, only the essential content of DIN 51309, which are crucial for highly precise torque transducers, are summarised below:

DOI: 10.5281/zenodo.8112428

- The torque measuring device comprises the transducer as well as other equipment like cables, slip rings, and housings, all of which must be clearly labelled.
- An overload test at 8 % to 12 % of the nominal torque for 1 to 1.5 min must be conducted.
- Temperature stabilisation / equalisation should be achieved by storing the device with applied supply voltage under calibration conditions.
- The zero signal of the unloaded transducer in a specific (vertical) position must be recorded before mounting.
- Mounting of the transducer should follow the manufacturer's specification.
- The ambient temperature should be stable to ± 1 K in the range of 18 °C to 28 °C and recorded.

The calibration procedure involves preloading and loads in different mounting positions. The load sequences include increasing and decreasing load steps. For the first mounting position, three preloads to the maximum torque are required, followed by an increasing, decreasing, and second increasing load sequence. Then, the transducer is rotated 120°, preloaded once with maximum torque, and subjected to an increasing and a decreasing load sequence. This last part (rotation-preload-load-sequences) is repeated once more. The DIN 51309 standard requires the calibration range to consist of equally spaced torque measurement points, with a minimum of eight torque steps distributed appropriately over the calibration range. The time between two consecutive torque levels should be as equal as possible, and the indicator reading should be taken after stabilisation (Figure 9).

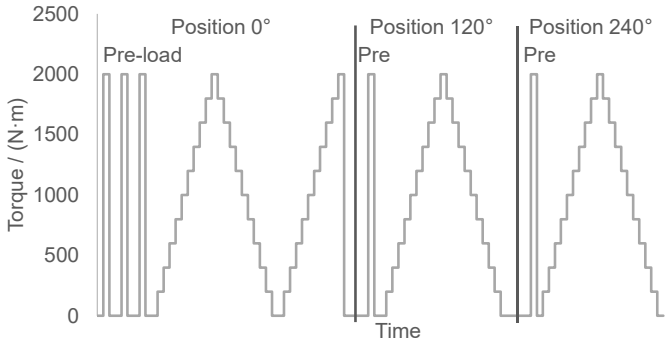

Figure 9: Example of rotation-preload-load-sequences, based on [9]**.**

Various parameters are computed to evaluate a transducer's performance after calibrating it. To begin with, the recorded values are corrected by taring them using the respective zero signal value obtained before the particular load sequence. The resulting corrected torque values are then utilised to determine the following:

- Calibration results Y and Y_h: The mean value of all mounting positions for the increasing load sequences (excluding the second increasing sequence for the first mounting position) calculated for every torque value.
- Reproducibility b: The largest deviation of the values from all mounting positions for the increasing load sequences calculated for every torque value.
- Repeatability b': The absolute deviation between the first and second increasing load sequences in the first mounting position calculated for every torque value.
- Zero point deviation f_0: The maximum absolute deviation between the zero values before and after an increasing-decreasing sequence (approximately 30 s after the last load has been relieved) calculated for each mounting position.
- Reversibility h: The maximum absolute deviation between the value of the increasing and decreasing load sequences in the same mounting position calculated for each torque value.
- Regression deviation f_a (indication deviation f_q): The deviation between the calibration results and the results of a third-degree fitting function (and the calibration torque), passing through the point of origin, calculated for each torque value.

These parameters are used either to classify the transducer or to determine the relative expanded MU. Additionally, DIN 51309 outlines a method for evaluating the transducer's short-term creep behaviour by computing the deviation of the zero signal before the first increasing load sequence and the zero signal after relieving the third preload, and dividing this by the calibration result for the maximum torque load. Furthermore, DIN 51309 permits continuous calibration, which differs from the standard calibration and evaluation process in that the preload duration is only 5 s. However, experimental investigations should be carried out to determine the impact of all conditions (e.g., display unit filter settings, torque increase velocity, etc.) on the MU before performing continuous calibration of a transducer.

2.4 Torque measurement under rotation – theoretical considerations

The aim of this task is to perform theoretical calculations of the influence of rotational speed on the torque measurement under constant rotation. This task is based on a real situation: rotation of the 5 MN m torque transducer (section 3.2) with the parameters given in **Table 1**.

Table 1: Specifications of the 5 MN m torque transducer and general specifications.

Specifications of the 5 MN m torque transducer		
Outer diameter	r_2	0.39XX m[1]
Inner diameter	r_1	0.32XX m
Length	L	0.6XXX m
Mass	m	1700 kg
Density	ρ	7XXX kg/m^3
Poisson's ratio	v	0.2XXX
E-modulus	E	1.XXXx10^{11} Pa
G-modulus	G	7.XXXx10^{10} Pa
k factor	k	2.0XXX
Supply voltage	U_E	5 V
General specifications		
Max. rot. speed	n_{max}	25 min^{-1}
Min. rot. speed	n_{min}	6.5 min^{-1}
Applied torque	M_T	1100 kN m

2.4.1 Theoretical calculations of the hollow shaft deformation – formulas

For the theoretical calculations, the transducer was simplified to a hollow cylinder with known dimensions r_1, r_2, and l.

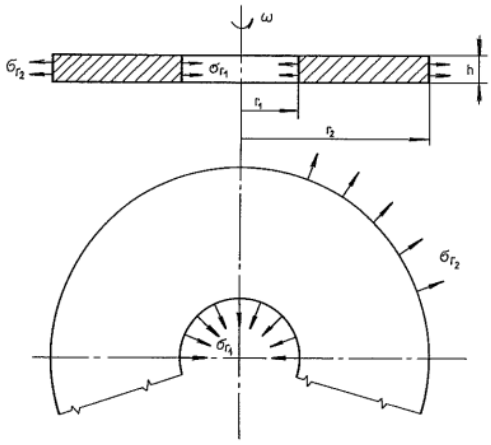

Figure 10: Hollow cylinder under rotation [10].

The change of the inner diameter r1, where the strain gauges are placed, is:

[1] Based on non-disclosure agreements with the transducer manufacturer, the exact figures cannot be given here.

DOI: 10.5281/zenodo.8112428

$$\Delta r_2 = \varepsilon_{t2} \cdot r_2 = \frac{r_2}{E}(\sigma_{t2} - \mu \cdot \sigma_{r2}) \quad (1)$$

$$\sigma_t(x) = C_1 + \frac{C_2}{x^2} - \frac{1+3\mu}{8} \cdot A \cdot x^2 \quad (2)$$

$$\sigma_r(x) = C_1 - \frac{C_2}{x^2} - \frac{3+\mu}{8} \cdot A \cdot x^2 \quad (3)$$

where C1 and C2 are constants derived from boundary conditions:

$$C_1 = \frac{3+\mu}{8} \cdot A \cdot (r_1^2 - r_2^2) \quad (4)$$

$$C_2 = \frac{3+\mu}{8} \cdot A \cdot (r_1^2 \cdot r_2^2) \quad (5)$$

And *A* is the influence of the centrifugal force:

$$A = \frac{\gamma}{g} \cdot \omega^2 = \rho \left(\frac{\pi \cdot n_{max}}{30}\right)^2 \quad (6)$$

2.4.2 Theoretical calculations of the hollow shaft deformation – results

The change of the outer diameter r_2 under maximum rotational speed n_{max} = 25 min^{-1}.

$$\Delta r_2 = \varepsilon_{t2} \cdot r_2 = \frac{r_2}{E}(\sigma_{t2} - \mu \cdot \sigma_{r2}) = 1.213 \cdot 10^{-8}\text{m} \quad (7)$$

$$\varepsilon = \frac{\Delta r_2}{r_2} = 3.09054 \cdot 10^{-8} \quad (8)$$

The transducer is deformed only in radial direction *r*, length *L* stays constant (*L* = const).

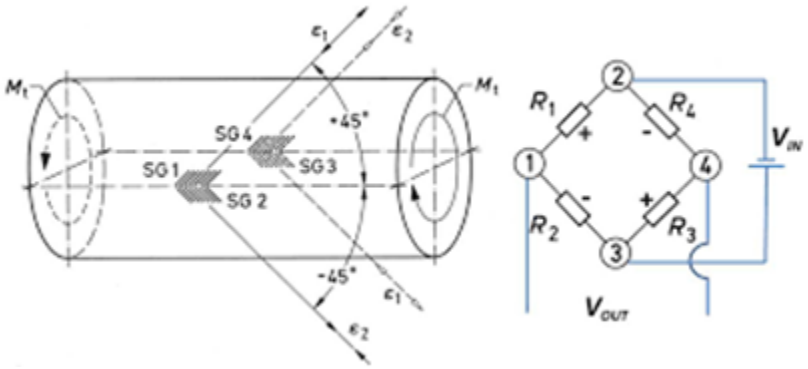

Figure 11: Set-up of the strain gauges in a torque transducer [10].

Deformation of the strain gauge according to the diameter change:

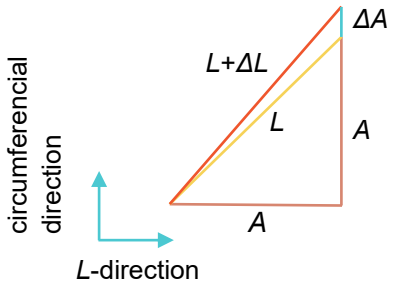

$$\varepsilon_{SG} = \frac{\Delta L}{L} = \frac{\sqrt{2 + 2\varepsilon + \varepsilon^2}}{\sqrt{2}} - 1 = 1.54527 \cdot 10^{-8} \quad (9)$$

2.4.3 Strain gauge signal calculation – loaded rotating transducer

The output strain gauge signal (change of resistance R) depends on the supply voltage U_E, and the change in the geometry. The formulas used are:

$$\frac{\Delta R}{R} = k \cdot \frac{\Delta \mathrm{L}}{L} = k \cdot \varepsilon \tag{10}$$

$$U_\mathrm{m} = U_\mathrm{n} \cdot \frac{\Delta R}{R} \tag{11}$$

$$\varepsilon = \frac{\Delta \mathrm{L}}{L} = \frac{\tau}{2 \cdot G} \tag{12}$$

$$U_\mathrm{m} = U_E \cdot k \cdot \frac{\Delta \mathrm{L}}{L} = U_\mathrm{E} \cdot k \cdot \frac{\tau}{2 \cdot G} \tag{6}$$

Because of the rotation, the geometry changes; so does the shear stress τ due to the change of the polar modulus J_P:

$$J_\mathrm{P} = \frac{\pi}{2}(r_2^4 - r_1^4) \tag{13}$$

$$\tau_\mathrm{max} = \frac{M_\mathrm{K}}{J_\mathrm{p}} \cdot r \tag{6}$$

The results for different rotational speeds from n_{min} = 0 min^{-1} to n_{max} = 100 min^{-1} for the 5 MN m torque transducer are given in Table 2.

Table 2: Theorical results for the 5 MN m torque transducer under rotation.

n / min^{-1}	$\varepsilon = \Delta R/R$	r_1 / m	r_2 / m	J_p / m^4	τ_{max} / Pa	U_m / V	S / mV/V
0	0	0.325	0.3925	0.01975539790	21854786	0.00144227379	0.2884547573
5	1.23621E-09	0.325000000371	0.39250000049	0.01975539801	21854786	0.00144227378	0.2884547561
10	4.94486E-09	0.325000001483	0.39250000194	0.01975539832	21854786	0.00144227376	0.2884547526
15	1.11259E-08	0.325000003337	0.39250000437	0.01975539884	21854786	0.00144227373	0.2884547468
25	3.09054E-08	0.325000009269	0.39250001213	0.01975540051	21854784	0.00144227364	0.2884547281
50	1.23621E-07	0.325000037075	0.39250004852	0.01975540834	21854777	0.00144227320	0.2884546405
100	4.94486E-07	0.325000148298	0.39250019409	0.01975543965	21854751	0.00144227145	0.2884542903

From the computed result can be assumed, that the influence of rotational speed on the torque measurement is hardly measurable. There is also another point of view: torque transducers are usually equipped with four strain gauges connected in a Wheatstone bridge. Those strain gauges are deformed in the same way as the transducer shaft changes symmetrically under rotation, so all four resistances R are the same. With this aspect, it can be assumed, that there should be no measurable change in the bridge caused by rotation. The same principle as for the thermal compensation can be applied. Imperfections in the system, such as imbalances, asymmetry, friction, inertial forces, etc., might cause measurable bridge changes.

DOI: 10.5281/zenodo.8112428

3 Standard calibrations

Contrary to what is required, a torque calibration under rotation is currently not possible. For this reason, four torque transducers were statically calibrated in the following and their behaviour when used under rotation was then analysed in different aspects. First, a torque transducer with a measurement range of up to 125 kN m to be used on the high-speed shaft of a wind turbine drive train, was calibrated statically and examined in a generator test bench at rotational speeds of up to 1500 min^{-1} using different data acquisition and filtering. Second, the 5 MN m torque transfer standard was calibrated up to 1.1 MN m and its calibration results were extrapolated up to 5 MN m as there are still no suitable calibration devices. Moreover, the transducer was used for torque measurement under rotation at rotational speeds up to 22.5 min^{-1}on a wind turbine drive train's low-speed shaft.

3.1 The T40FH

The T40FH is a torque transducer for usage under rotation made by HBK. It is ideal for power test benches and offshore industry tests covering nominal torque values from 100 kN m to 300 kN m, with maximum permissible rotational speeds ranging from 2000 to 3000 min^{-1} depending on the model. An integrated magnetic rotational speed measuring system with 72/86 pulses per revolution is available as an option. In the HiL-GridCoP generator test bench [11] at Fraunhofer Institute for Wind Energy Systems (IWES) in Bremerhaven, Germany, a T40FH torque transducer with a nominal torque value of 125 kN m is assembled.

Figure 12: T40FH torque transducer manufactured by HBK [12].

Calibration up to 125 kN m

The torque transducer T40FH was calibrated up to 125 kN m using PTB's 1.1 MN m reference TSM. When a linear regression for increasing torque (case I in DIN 51309) is used to show the sensitivity of the T40FH, the relative expanded MU U (k = 2) ranges from 0.081 % at 125 kN m to approximately 0.14 % in the lower measurement range. The linear regression equation for increasing torque (case I) is provided as:

for clockwise torque $$S_{\mathrm{ai}} = 0.9616 \cdot M_{\mathrm{i}}, \quad (14)$$
for anti-clockwise torque $$S_{\mathrm{ai}} = 0.96188 \cdot M_{\mathrm{i}}, \quad (15)$$
for both combined $$S_{\mathrm{ai}} = 0.96174 \cdot M_{\mathrm{i}}, \quad (16)$$

where S_{ai} is the output signal in mV/V and M_i is the torque load in kHz.

The creep influence based on the short-term creep multiplied by four yields 0.007 %. A detailed explanation about creep influence from short-term creep can be found in [13].

Linearity deviation

A common method for representing torque calibration is by plotting the linearity deviation of the measured load curves relative to the sensitivity at maximum torque load, as shown in Figure 13. This representation allows for the derivation of other parameters such as hysteresis / reversibility *h*, zero point deviation f_0, repeatability *b'*, and reproducibility *b*. It is observed that the relative linearity deviation and thereby the hysteresis are not around zero as usual, but in the range between 0 and $-1.5 \cdot 10^{-4}$. For clockwise torque, the relative repeatability is further below the $2.5 \cdot 10^{-4}$ limit for class 0.05 at a maximum of $6 \cdot 10^{-5}$. For the anti-clockwise torque, on the other hand, even the limit value of 0.05 for class 0.1 is exceeded. A similar behaviour can be seen for the relative reproducibility, with class 0.05 being achieved for the clockwise torque and only class 0.1 for the anti-clockwise torque. Both the relative zero point deviation and the relative reversibility are below the respective limit values.

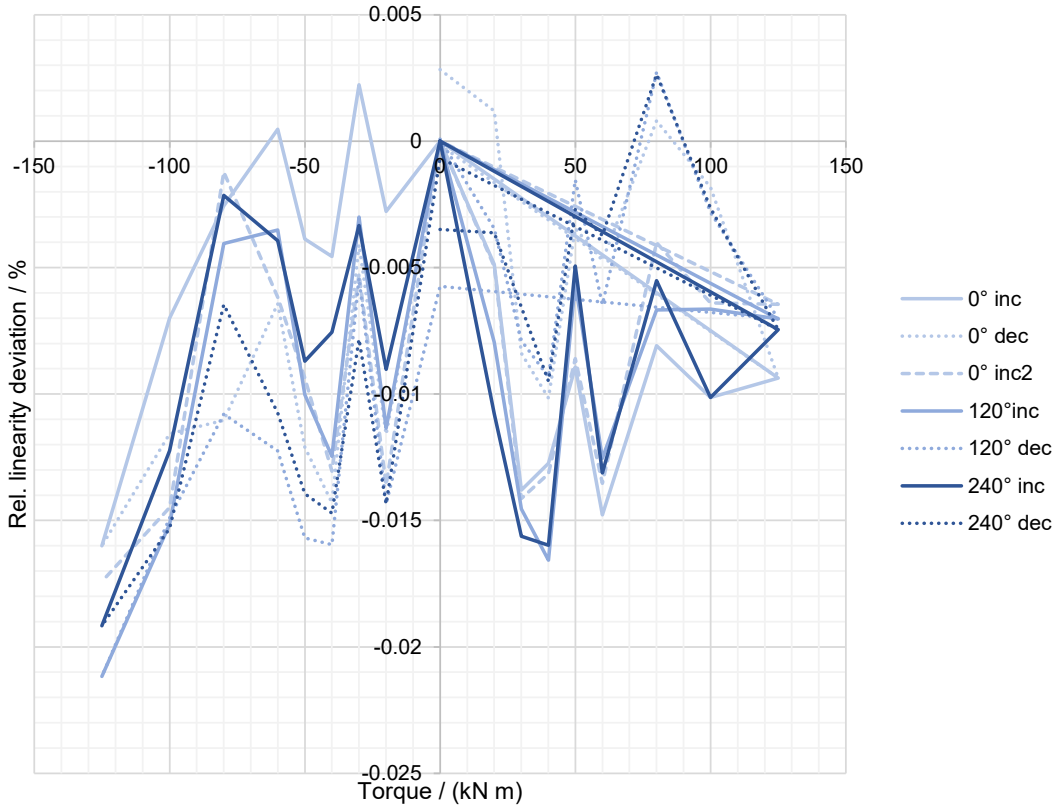

Figure 13: Relative linearity deviation of the 125 kN m torque transducer T40FH for clockwise and anti-clockwise torque.

Regression deviation

The relative regression deviation (Figure 14) is the difference between the calibration result and fitted (cubic (only increasing load steps), linear (only increasing load steps), and linear II (increasing and decreasing load steps)) calibration curve relative to the calibration result. The regression deviation of between -0.04 % and 0.05 % for all three fitting approaches lies within the expected range.

DOI: 10.5281/zenodo.8112428

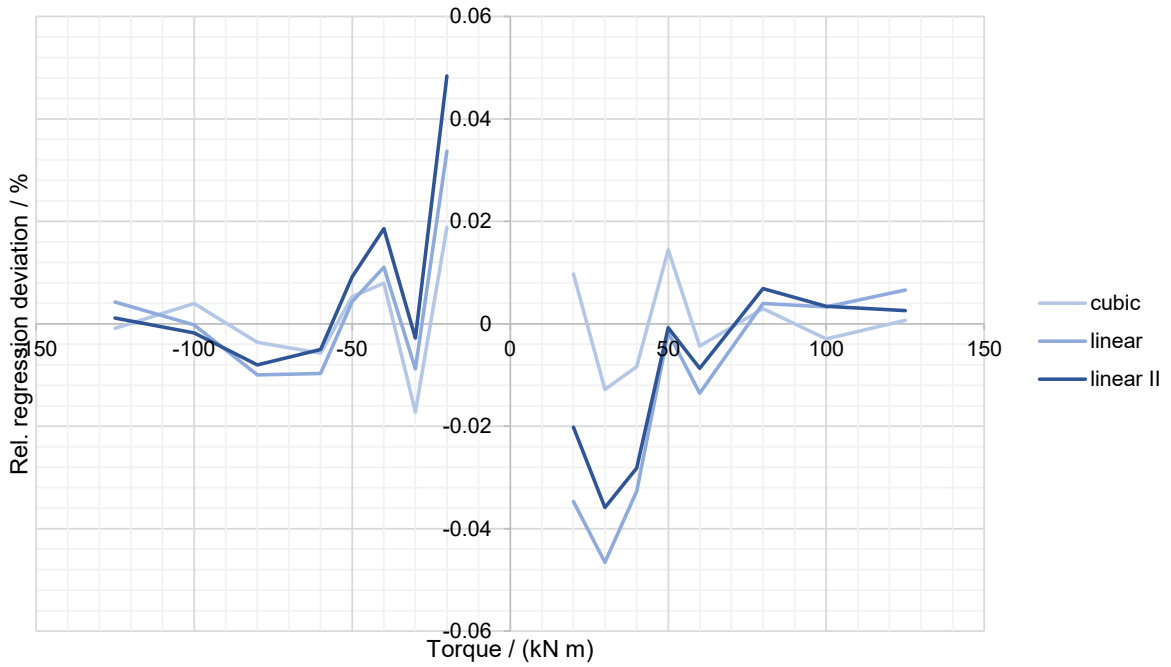

Figure 14: Relative regression deviation of the 125 kN m torque transducer T40FH for clockwise and anti-clockwise torque.

Relative expanded measurement uncertainty

For the 125 kN m torque transducer, the relative expanded MU interval (k = 2) for all three fitting cases is given in Table 3.

Table 3: Relative expanded MU interval (k = 2) of the 5 MN m torque transducer for the calibration performed in 2020.

Steps kN m	cubic %	linear %	linear II %
-125	0.080	0.081	0.081
-100	0.080	0.080	0.085
-80	0.100	0.102	0.115
-60	0.101	0.102	0.115
-50	0.101	0.101	0.120
-40	0.102	0.105	0.136
-30	0.103	0.104	0.118
-20	0.112	0.130	0.188
0	-	-	-
0	-	-	-
20	0.102	0.124	0.145
30	0.010	0.137	0.155
40	0.100	0.120	0.140
50	0.100	0.100	0.108
60	0.100	0.104	0.119
80	0.100	0.100	0.114
100	0.080	0.080	0.089
125	0.080	0.081	0.083

3.2 The 5 MN m torque transducer

The 5 MN m torque transducer (Figure 15) is a customised flange type torque transducer developed and manufactured by HBK based on the SG principle. The torque transducer with a diameter of approx. Ø 1200 mm and measuring hollow shaft length of approx. 600 mm has a nominal torque sensitivity of 1.75 mV/V at 6 MN m, an axial force sensitivity of 1.69 mV/V at 30 MN, a shear force sensitivity of 1.79 mV/V at 8 MN and a bending moment sensitivity of 1.58 mV/V at 3 MN m. It can be deployed within a temperature range from 10° C to 60° C. The transducer was developed for torque measurement under rotation in wind turbines and special system test bench for wind turbine drive trains. For this mission, it was also equipped with a telemetry system for data transmission.

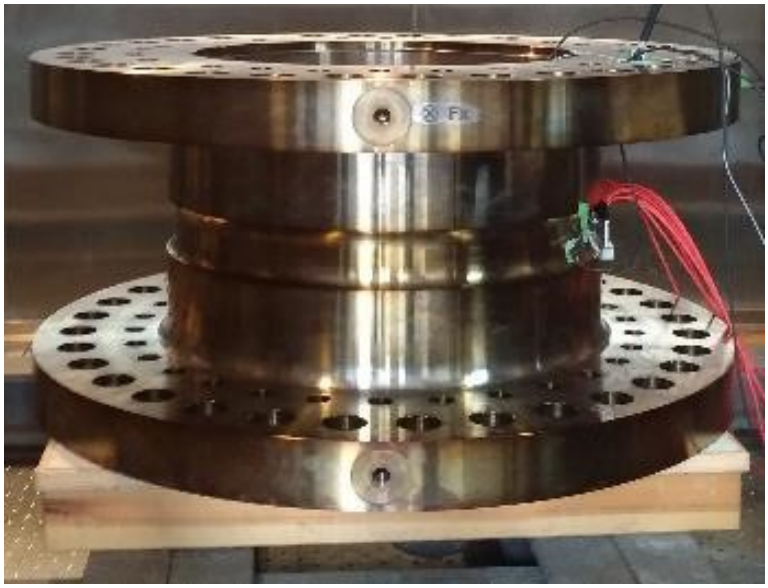

Figure 15: 5 MN m torque transducer with additional bridges to measure bending moments and longitudinal and lateral forces.

Previously, the 5 MN m torque transducer could only be calibrated up to 1.1 MN m due to the lack of calibration devices with a larger calibration range (cf. section 2.2). Calibration was carried out according to DIN 51309 in both clockwise and anti-clockwise directions. To better characterise the transducer, partial range calibrations were performed up to 600 kN m and 800 kN m.

3.2.1 Calibration up to 1.1 MN m

When a linear regression for increasing torque (case I in DIN 51309) is used to show the sensitivity of the 5 MN m torque transducer, the relative expanded MU interval U (k = 2, linear case II) ranges from 0.08 % at 1.1 MN m to approximately 0.17 % in the lower measurement range. The transducer is classified as class 0.5 due to the relative expanded MU of the calibration device (U = 0.08 % (k = 2)). The classification criteria are significantly below the limits for class 0.05, especially for anti-clockwise torque, except for the linear regression deviation. For measuring bridge M_{z1}, the linear regression equation for increasing torque (case I) is also provided:

for clockwise torque $$S_{\mathrm{ai}} = 0.00025974 \cdot M_{\mathrm{i}}, \quad (17)$$
for anti-clockwise torque $$S_{\mathrm{ai}} = 0.00025971 \cdot M_{\mathrm{i}}, \quad (18)$$
for both combined $$S_{\mathrm{ai}} = 0.00025973 \cdot M_{\mathrm{i}}, \quad (19)$$

where S_{ai} is the output signal in mV/V and M_i is the torque load in kN m.

Linearity deviation

The linearity deviation of the 5 MN m torque transducer up to 1.1 MN m is shown in Figure 16. For the 5 MN m torque transducer, it is observed that the hysteresis remains consistently around $2 \cdot 10^{-5}$ for clockwise torque across all partial range calibrations. This is contrary to what is expected based on

DOI: 10.5281/zenodo.8112428

literature, which predicts a scaling of the maximum torque. Additionally, it is noted that the linearity deviation does not vary for each sub-range and does not exhibit the expected scaling behaviour.

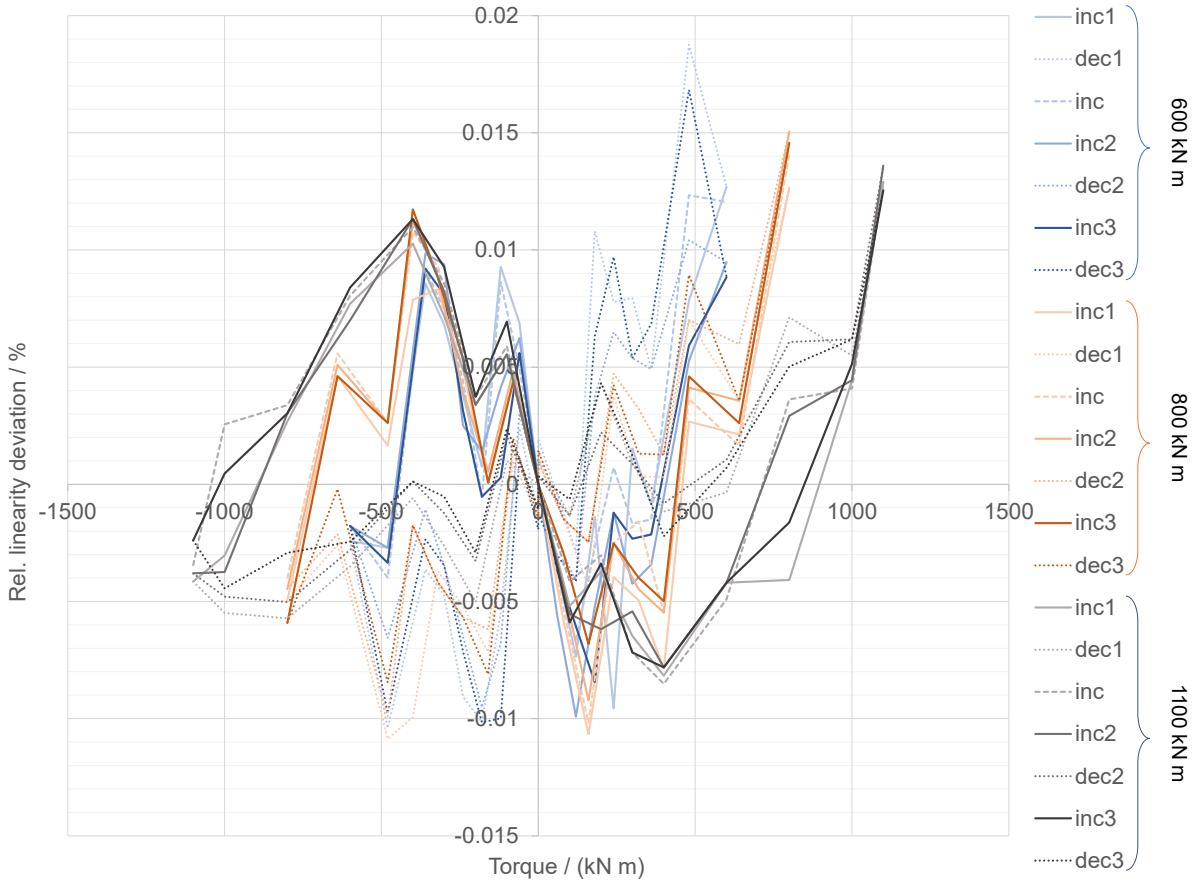

Figure 16: Relative linearity deviation of the 5 MN m torque transducer for clockwise and anti-clockwise torque up to 600 kN m, 800 kN m, and 1100 kN m.

Regression deviation

The relative regression deviation of the 5 MN m torque transducer (Figure 17) for cubic, linear, and linear II fitting curves ranges between -0.08 % and 0.02 % and is thus below the limit of ±0.05 % relative regression deviation for class 0.1.

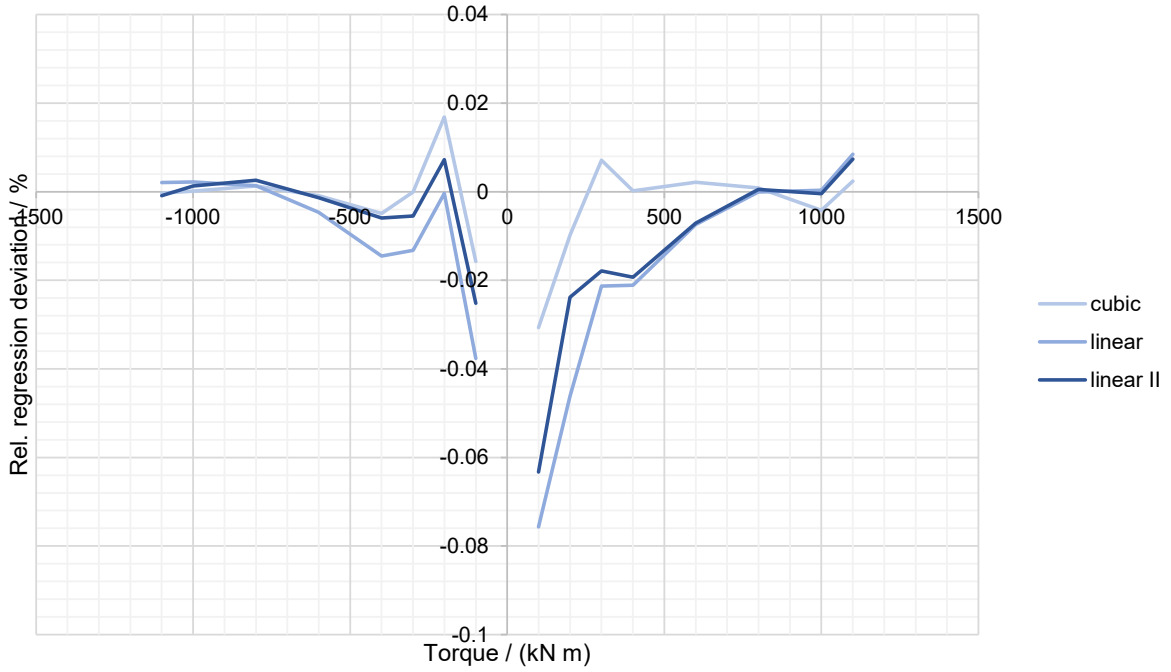

Figure 17: Relative regression deviation of the 5 MN m torque transducer for clockwise and anti-clockwise torque up to 1.1 MN m.

Drift of unmounted zero signal

The stability of the transducer's zero signal in unmounted state over the project duration (roughly 2020 – 2023) is shown in Figure 18. The stability of the zero signal in unmounted state is determined as the relative deviation of each mV/V signal from their arithmetic mean. Between the first calibration in 2020 and the second calibration in 2022, the transducer was mounted in the 10 MW nacelle system test bench DyNaLab at Fraunhofer IWES in Bremerhaven and loaded up to 5 MN m for the first time. In 2022, after the second calibration and before the third calibration in 2023, the 5 MN m torque transducer was installed in the 4 MW nacelle system test bench at the Center For Wind Power Drives (CWD) Aachen of RWTH Aachen University and loaded up to 1.5 MN m.

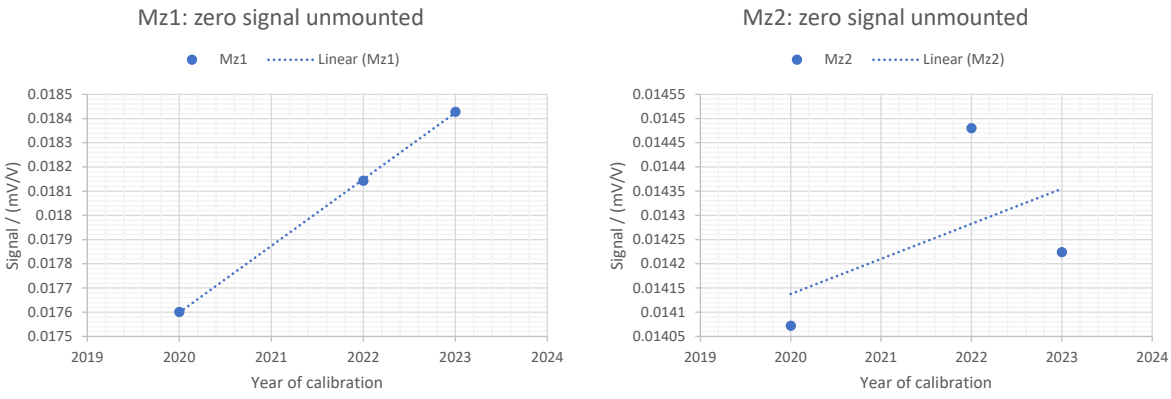

Figure 18: Relative deviation of each zero signal in unmounted state from their mean value for the two torque bridges M_{z1} and M_{z2} of the 5 MN m torque transducer.

The zero signal drift of the transducer in unmounted state for measuring bridge M_{z1} is linear over time, while the zero signal drift of measuring bridge M_{z2} is more randomly distributed. The total signal drift between 2020 and 2023 for measuring bridge M_{z1} amounts to 0.8267 nV/V, for the measuring bridge M_{z2}, it is 0.1517 nV/V.

DOI: 10.5281/zenodo.8112428

Sensitivity drift

Like the drift of unmounted zero signal, the sensitivity drift (Figure 18) is determined as the relative deviation of each sensitivity value from their arithmetic mean. For both measuring bridges, a nearly linear drift over time can be observed. Moreover, both measuring bridges drift by the same amount.

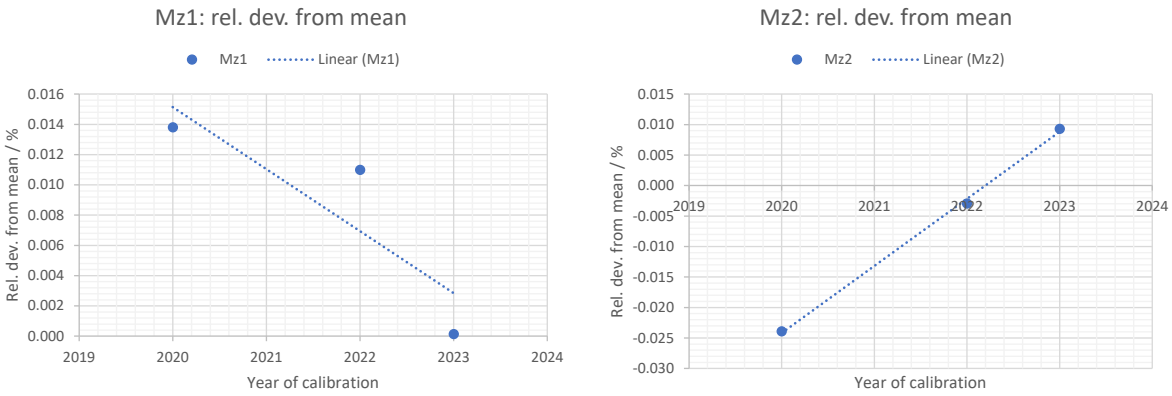

Figure 19: Relative deviation of each sensitivity value from their mean value for the two torque bridges M_{z1} and M_{z2} of the 5 MN m torque transducer.

Relative expanded measurement uncertainty

For the 5 MN m torque transducer, the relative expanded MU interval (k = 2, Table 4) for all three fitting cases is given exemplarily for the calibration in 2020.

Table 4: Relative expanded MU interval (k = 2) of the 5 MN m torque transducer for the calibration performed in 2020.

Steps	M_{z1}			M_{z2}		
kN m	cubic / %	linear / %	linear II / %	cubic / %	linear / %	linear II / %
-1100	0.080	0.080	0.081	0.080	0.080	0.083
-1000	0.080	0.080	0.084	0.080	0.080	0.083
-800	0.080	0.080	0.087	0.080	0.080	0.088
-600	0.080	0.081	0.089	0.080	0.081	0.092
-400	0.080	0.085	0.104	0.080	0.080	0.105
-300	0.080	0.084	0.097	0.080	0.085	0.100
-200	0.080	0.080	0.103	0.080	0.080	0.111
-100	0.081	0.110	0.127	0.083	0.119	0.169
0	-	-	-	-	-	-
0	-	-	-	-	-	-
100	0.081	0.171	0.161	0.081	0.166	0.156
200	0.083	0.124	0.137	0.080	0.144	0.144
300	0.080	0.091	0.106	0.080	0.097	0.111
400	0.080	0.090	0.104	0.080	0.089	0.102
600	0.080	0.081	0.090	0.080	0.086	0.100
800	0.080	0.080	0.085	0.080	0.080	0.086
1000	0.080	0.080	0.081	0.080	0.081	0.086
1100	0.080	0.082	0.087	0.080	0.081	0.085

3.2.2 Measurement and extrapolation up to 5 MN m

Three approaches for extrapolating the MU of a partial range calibration are shown below. In the first approach, the calibration process utilises the linear regression method and weighted least squares

method (WLS) to determine the linear relationship between the electric signal ant torques based on measured data points. The uncertainties were considered, and the results of applying WLS and the Monte Carlo Method (MCM) are presented. In the second approach the worst uncertainty per class as stipulated in DIN 51309 is used for the extrapolated range. This approach is refined by the third approach, which…

Approach 1 – Janusz Fidelus, Jacek Puchalski

The studies were carried out for the 5 MN m torque transducer located in PTB and calibrated in PTB up to 1.1 MN m – in further studies marked as "**Case I**". The symbols used and the analyses carried out were performed in accordance with the Guide to the Expression of Uncertainty in Measurement (GUM) [15]. These analyses will be presented in [16].

Calibration of the torque transducer to the electric signal

The linear regression method is used to determine the linear dependence of the electric signal y as the function of torques x based on n measurement points. The WLS minimises the sum of squares of errors normalised to the variances along the axis OY, since the uncertainties of the x-coordinate are negligible and also there is no correlations at any pairs of measured coordinates. The measurements were carried out at points with coordinates x_i, y_i (i = 1,…,n), where standard uncertainties relate only to the measurement of the signal and $u(y_i) = y_i \cdot \delta(y_i)/100$, whereby $\delta(y_i)$ of the standard relative uncertainties of the signal is denoted. The data for **Case I** are given in Table 5.

Table 5: Input data for straight line regression – results from measurements for Case I [17].

Torque x / (kN m)	Case I (up 1.1 MN m)	
	Signal y / (mV/V)	Measure of rel. standard uncertainty of signal $\delta(y)$ / %
Clockwise torque		
0	0.013913	
100	0.025956	0.166
200	0.051919	0.144
300	0.077903	0.097
400	0.103879	0.089
600	0.155825	0.086
800	0.207793	0.080
1000	0.259765	0.081
1100	0.285745	0.081
Anticlockwise torque		
-1100	-0.285722	0.080
-1000	-0.259750	0.080
-800	-0.207792	0.080
-600	-0.155834	0.081
-400	-0.103900	0.080
-300	-0.077912	0.085
-200	-0.051949	0.080
-100	-0.025986	0.119
0	0.013913	

Linear equation $y = ax + b$ coefficients a and b and the standard uncertainties of the ratios u_a and u_b and the correlation coefficient are expressed by the following formulae:

$$a = \frac{\Delta_a}{\Delta}, b = \frac{\Delta_b}{\Delta}, u_a = \sqrt{\frac{S}{\Delta}}, u_b = \sqrt{\frac{S_{xx}}{\Delta}}, \rho_{ab} u_a u_b = -\frac{S_x}{\Delta} \quad (20)$$

where

$$\Delta = S \cdot S_{xx} - S_x^2, \Delta_a = S \cdot S_{xy} - S_x \cdot S_y, \Delta_b = S_y \cdot S_{xx} - S_x \cdot S_{xy} \quad (21)$$

DOI: 10.5281/zenodo.8112428

and the auxiliary variables are given by:

$$S = \sum_{i=1}^{n} \frac{1}{u^2(y_i)}, S_{\mathrm{x}} = \sum_{i=1}^{n} \frac{x_i}{u^2(y_i)}, S_{\mathrm{xx}} = \sum_{i=1}^{n} \frac{x_i^2}{u^2(y_i)}, S_{\mathrm{xy}} = \sum_{i=1}^{n} \frac{x_i y_i}{u^2(y_i)}, S_{\mathrm{y}} = \sum_{i=1}^{n} \frac{y_i}{u^2(y_i)} \quad (22)$$

In the case of a straight line regression defined by the uncertainty equation, the $y = ax + b$ standard uncertainty for a regression line along OY is defined by the formula:

$$u_{\mathrm{y}}^2 = u_{\mathrm{a}}^2 + 2|x|u_{\mathrm{a}}u_{\mathrm{b}}\rho_{\mathrm{ab}} + u_{\mathrm{b}}^2, \quad (23)$$

according to the law of propagation of uncertainty (LPU) as the sum of distributions in general correlated variables ax with a standard uncertainty $|x|u_{\mathrm{a}}$ and the distribution of variable b with a standard uncertainty u_{b}, where ρ_{ab} is the correlation coefficient between these random variables. The expanded uncertainty for a straight line regression is increased by the coverage factor determined by the inverse distribution function from the Student's t-distribution with n-2 degrees of freedom for a coverage of 0.95 (α = 0.05) is:

$$U_{\mathrm{y}} = t_{n-2,1-a/2}u_{\mathrm{y}}. \quad (24)$$

The uncertainty area of the regression line is described by $y = ax + b \pm U_{\mathrm{y}}$.

In the case of the MCM, random variables corresponding to the abscissae of the measurement points are generated in the form of samplings (10^7 samples drawn) from Gaussian distributions $N(\mu,\sigma^2)$ with expected values $\mu = y_i$ and variances $\sigma^2 = u^2(y_i)$ i = 1,…,n.

The values of the coverage corridor are intervals for 0.95 probability of the selected x and are determined by the sum of the $ax + b$ distributions, using formulae defining parameters of slope a and intercept b as described above.

The results of the data after applying WLS and MCM for Case I are collected in Table 6 and Figure 20 to Figure 23.

Table 6: Results of the straight line regression-linear characteristics of the 5 MN m torque transducer (Case I).

Torque x / (kN m)	Case I (up to 1.1 MN m)		
	Signal y / (mV/V) a = 2.5977E-04 / (mV/V / kN m) b = -2.6088E-05 / (mV/V)	Exp. rel. uncertainty of signal δ / %	
		LPU k = 2.45	MCM
Clockwise torque			
100	0.02595	0.1698	0.1358
200	0.05193	0.0720	0.0577
300	0.07791	0.0473	0.0379
400	0.10388	0.0412	0.0329
600	0.15584	0.0419	0.0335
800	0.20779	0.0451	0.0360
1000	0.25975	0.0475	0.0380
1100	0.28572	0.0485	0.0388
1200	0.31170	0.0495	0.0395
1600	0.41561	0.0519	0.0416
2000	0.51952	0.0537	0.0430
4000	1.03907	0.0573	0.0458
8000	2.07816	0.0593	0.0474
10000	2.59770	0.0595	0.0477
12000	3.11725	0.0598	0.0479

16000	4.15634	0.0600	0.0481
20000	5.19544	0.0603	0.0483
24000	6.23453	0.0605	0.0484
30000	7.79317	0.0605	0.0485
32000	8.31271	0.0605	0.0485
40000	10.39090	0.0608	0.0486
50000	12.98863	0.0608	0.0487
60000	15.58636	0.0608	0.0487
80000	20.78182	0.0610	0.0488
100000	25.97728	0.0610	0.0488
Anticlockwise torque			
a, b	*a* = 2.5972E-04 / (mV/V / kN m) ; *b* = - 9.569E-06 / (mV/V); *k* = 2.45		
-90000	-23.374784	0.0556	0.0445
-5000	-12.985995	0.0555	0.0444
-4800	-5.194404	0.0552	0.0441
-4000	-2.597207	0.0546	0.0436
-3000	-2.077767	0.0543	0.0434
-2500	-1.298608	0.0534	0.0427
-2000	-0.519449	0.0501	0.0400
-1600	-0.415561	0.0487	0.0390
-1100	-0.285701	0.0459	0.0367
-1000	-0.259729	0.0450	0.0360
-800	-0.207785	0.0428	0.0342
-600	-0.155841	0.0397	0.0317
-400	-0.103897	0.0364	0.0291
-300	-0.077925	0.0376	0.0300
-200	-0.051954	0.0511	0.0409
-100	-0.025982	0.1201	0.0960

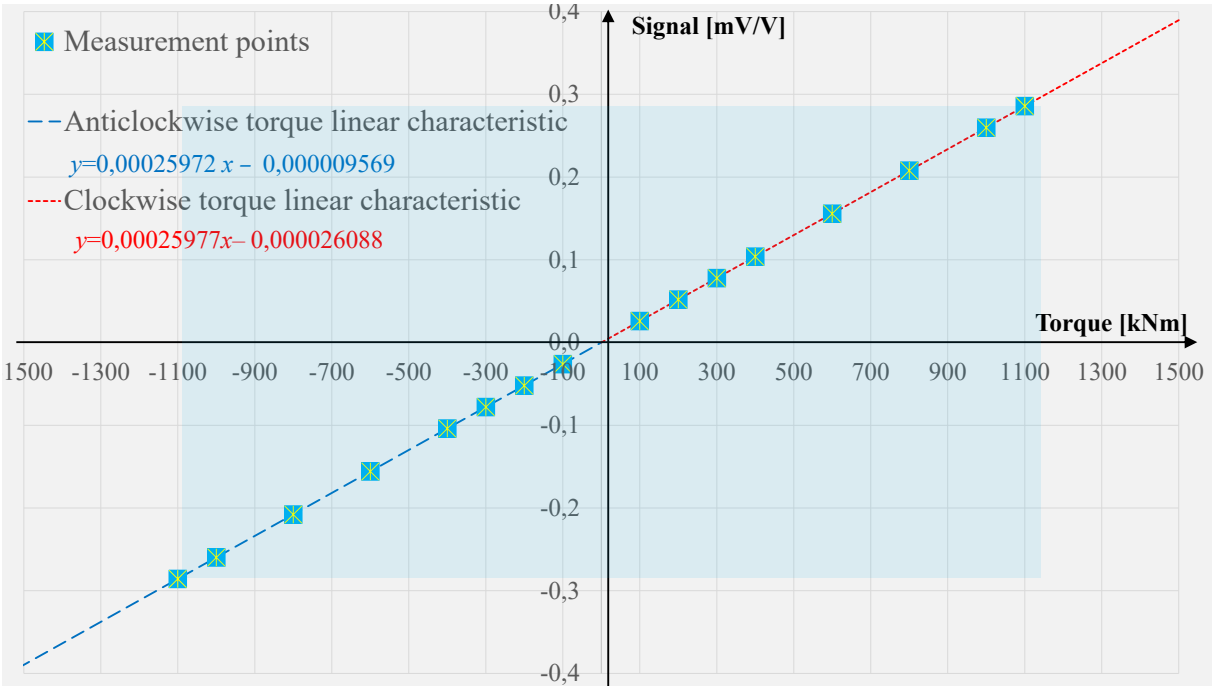

Figure 20: Calibration characteristics with measurement points and calibration area for Case I, results from Table 6.

DOI: 10.5281/zenodo.8112428

The extrapolation of linear characteristics of the normalised signal from the torque transducer was performed as a function of torque in the range from -100 MN m up to 100 MN m, illustrating this in Figure 21.

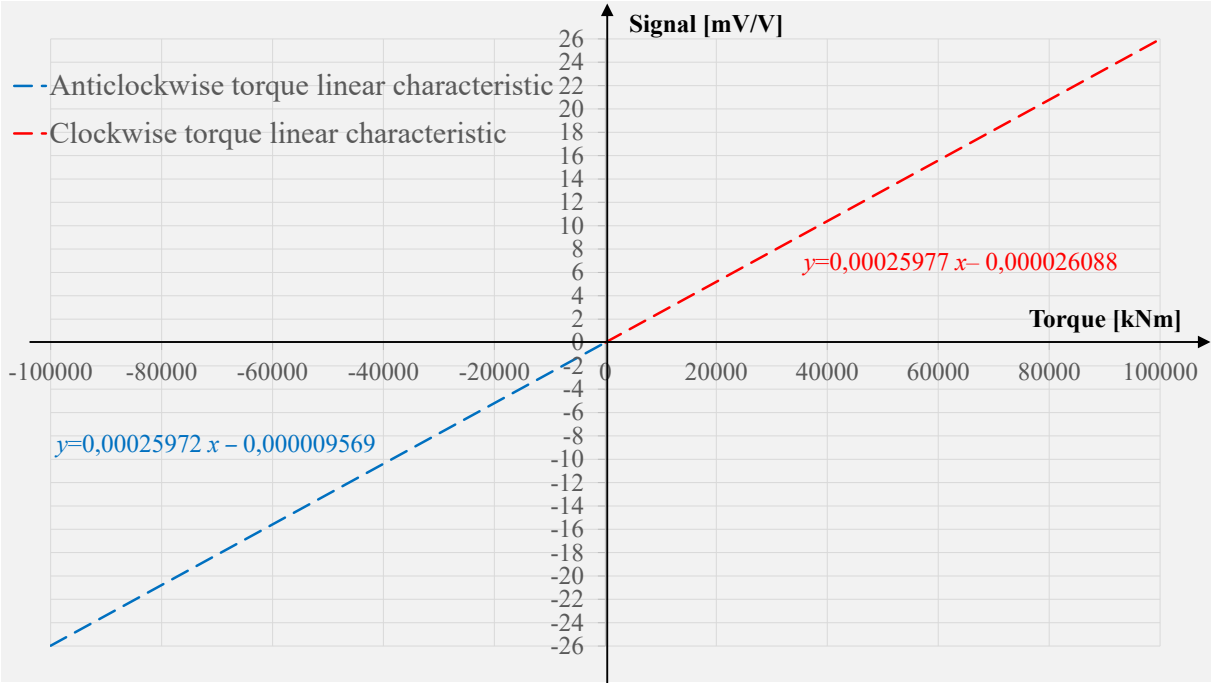

Figure 21: Extrapolation of calibration characteristics outside of the measurement area for Case I, results from Table 6.

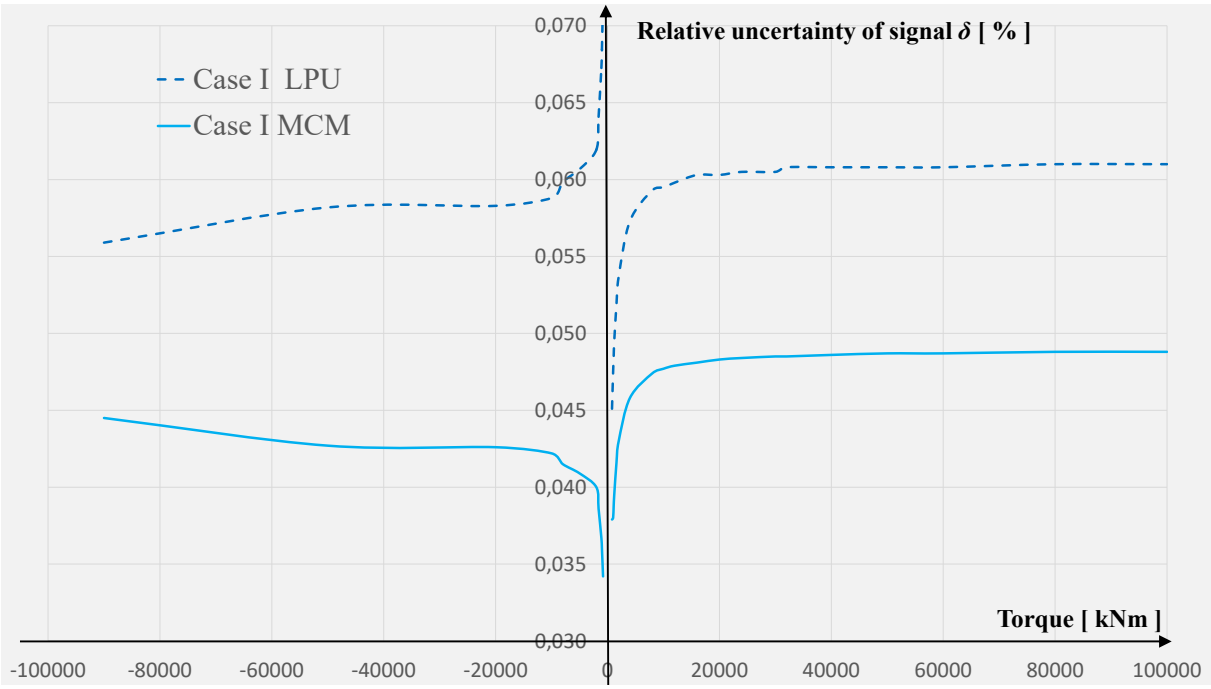

Figure 22: Relative uncertainty of the signal for Case I, results from Table 6.

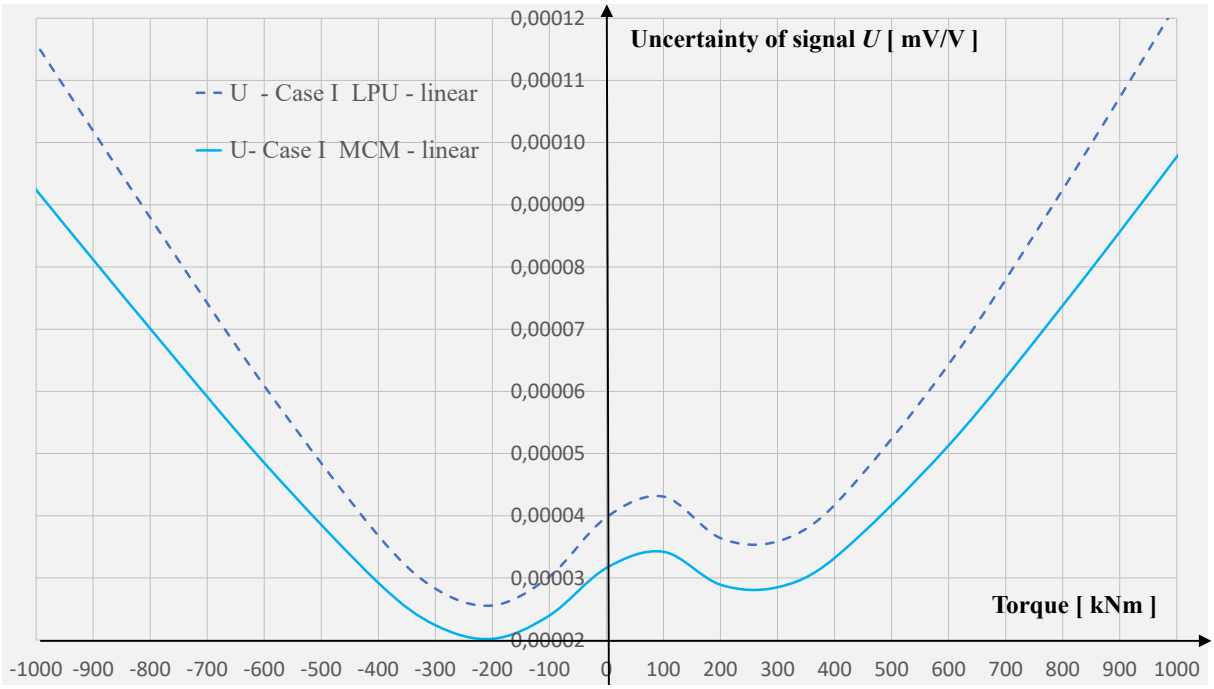

Figure 23: Absolute uncertainty of the signal for Case I, results from Table 6.

In addition, matching to the measured coordinates was performed with cubic splines, i.e., polynomials of the third degree, which, due to their characteristics, can adjust to various types of nonlinearities. In interpolating problems, cubic spline interpolation is often preferred to other polynomial of higher degree. But this interpolation, in general, cannot be used for the analytic continuation – extrapolation of characteristics by cubic spline on the not-measured range of the instrument, e.g., the torque transducer. Additionally, the expanded uncertainties estimated from the MCM for all cases are much higher for a cubic spline than for linear interpolation.

Approach 2 – Rafael Soares de Oliveira

This extrapolation approach is called "worst uncertainty per class". To give an idea of the uncertainty magnitudes through the classes' ranges as given in DIN 51309, in each class range the worst expanded relative MU W (Case I-A) is calculated by combining the uncertainty contributions based on the maximum permissible error of each parameter:

$$W_{\mathrm{wCM}} = 2 \cdot \sqrt{w_{\mathrm{b}}^2(Y) + w_{\mathrm{b}'}^2(Y) + 2 \cdot w_r^2(Y) + w_0^2(Y_{\mathrm{E}}) + w_{\mathrm{fa}}^2(Y) + w_{\mathrm{CM}}^2(Y)}, \tag{25}$$

$$W_{\mathrm{woCM}} = 2 \cdot \sqrt{w_{\mathrm{b}}^2(Y) + w_{\mathrm{b}'}^2(Y) + 2 \cdot w_r^2(Y) + w_0^2(Y_{\mathrm{E}}) + w_{\mathrm{fa}}^2}, \tag{26}$$

where w_{b} is the relative standard deviation of the reproducibility b, $w_{\mathrm{b}'}$ of the repeatability b', w_{r} of the resolution r, w_0 of the zero point deviation f_0, w_{fa} the one of the regression deviation f_{a}, and w_{CM} of the calibration machine (CM). All standard deviations are given in %. In Table 7, the relative quantities of the classification criteria as stated in DIN 51309 are presented. The rel. exp. MUs W_{wCM} and W_{woCM} indicate the measured quantity of the torque transducer's output signal Y in mV/V. In order to be able to calculate the rel. exp. MU based on the maximum classification parameters using LPU, it must be assumed that Y_{E} and Y are virtually identical signal measurement values.

DOI: 10.5281/zenodo.8112428

Table 7: Classification characteristics (Case I-A) of torque measuring devices acc. to DIN 51309 [9].

class	Maximum permitted values of the parameter / %						Lower limit of the measurement range	rel. MU of the calibration torque (CM)	*W* without CM / %	*W* with CM / %
	b/Y	b'/Y	f_0/Y_E^2	h/Y		f_q/Y and f_a/Y				
0.05	0.05	0.025	0.0125	0.063	±	0.025	0.00400	0.01	0.035	0.036
0.1	0.1	0.05	0.025	0.125	±	0.05	0.00200	0.02	0.069	0.072
0.2	0.2	0.1	0.05	0.25	±	0.1	0.00100	0.04	0.138	0.144
0.5	0.5	0.25	0.125	0.63	±	0.25	0.00040	0.1	0.346	0.360
1	1	1	0.25	1.25	±	0.5	0.00020	0.2	0.854	0.877
2	2	2	0.5	2.5	±	1	0.00010	0.4	1.708	1.754
5	5	5	1.25	6.25	±	2	0.00004	1	4.225	4.342

In Figure 24, the worst rel. exp. MU per class without rel. MU of the calibration torque W_{woCM}, which is in most cases the rel. exp. MU of the TSM used, is depicted. As a very simple approach to extrapolation, the worst rel. exp. MU for the class specified in the calibration certificate for the partial range calibration can be used. However, this method does not take into account the uncertainty of the extrapolation itself, which is just a prediction and should also be associated with an uncertainty.

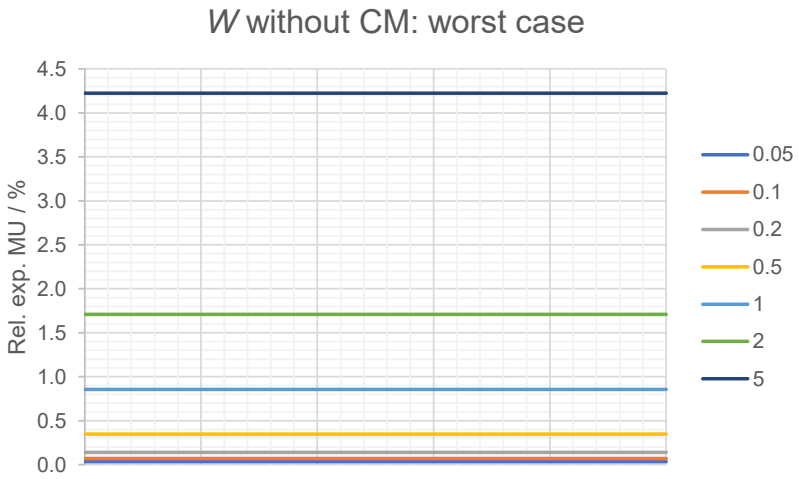

Figure 24: Worst rel. exp. MU per class without rel. MU of the calibration torque (rel. exp. MU of the TSM).

Approach 3 – Paula Weidinger

In this method for calibration result extrapolation, the linear regression curve determined in the partial range is used for converting the mV/V signal into the corresponding torque value. To validate this procedure, a 20 kN m torque transducer was measured in three partial (20 %, 50 %, and 80 %) and in the full range, and the relative sensitivities per calibration range were compared. These absolute differences are in the range of about $3x10^{-6}$ and thus smaller than the MU of the calibration itself, which is $3x10^{-5}$ for case I-A (cubic, smallest MU). The use of linear regression curves, which were determined in the partial range, in the full range is therefore legitimate. In order to check the 5 MN m torque transducer's sensitivity stability, it was calibrated in further sub-ranges (8 %, 12 %, 16 %, and 22 %) and the results were compared with each other. The absolute difference in range sensitivity is about $8x10^{-8}$

[2] In order to be able to calculate the rel. exp. MU based on the maximum classification parameters using LPU, it must be assumed that Y_E and Y are virtually identical signal measurement values.

DOI: 10.5281/zenodo.8112428

and thus noticeably smaller than the overall uncertainty of the calibration, which is 8×10^{-4} for the best case I-A.

The extrapolation approach described below is a prediction of the MU in a non-calibrated measurement range comparable to [18]. The method does not replace calibration and should only be used when calibration is not possible. With this extrapolation approach, the MU of the maximum calibration torque in the sub-range is multiplied by a prediction or extrapolation factor that is intended to take the uncertainty of the extrapolation itself into account. There are different calculation approaches for this factor:

- a simple scaling factor f_s calculated from the ratio of the extrapolated torque M_{ex} step to the maximum torque of the partial range calibration:

$$f_s = \frac{M_{ex}}{M_C}; \tag{27}$$

where M_C is the calibration sub-range.

- for a weighted scaling factor f_w, the simple scaling factor f_s is supplemented with an additional contribution based on the class of the partial range calibration:
  - one weighting factor f_{w1} is the sum of the scaling factor f_s and the expanded relative MU W of the class assigned to the transducer in the sub-range calibration:

$$f_{w1} = f_s + W_{CMC}, \tag{28}$$

  - the second weighting factor f_{w2} is the sum of the scaling factor f_s and the classification criteria (cf. Table 7) of the class determined in the partial range calibration:

$$f_{w2} = f_s + \frac{b}{Y} + \frac{b'}{Y} + \frac{f_0}{Y} + \frac{h}{Y} + \frac{f_a}{Y} + M_A + W_{wCM}, \tag{29}$$

where Y is the calibration result, M_A the lower limit of the measurement range depending on the resolution r of the torque transducer, and W_{wCM} the rel. exp. MU of the calibration torque.

Table 8 lists the scaling factor and the weighting factors for the 5 MN m transducer and the extrapolated rel. exp. MU using the different prediction factors.

DOI: 10.5281/zenodo.8112428

Table 8: **Scaling and weighting factors for the 5 MN m torque transducer calibrated in the sub-range up to 1.1 MN m and extrapolated rel. exp. MU for the range between 1.5 MN m and 5 MN m.**

torque	factors			extrapolated rel. exp. MU / %		
steps	f_s	f_{w1}	f_{w2}	f_s	f_{w1}	f_{w2}
-5000	4.5	4.9	6.4	0.38	0.40	0.53
-4500	4.1	4.5	5.9	0.34	0.37	0.49
-4000	3.6	4.0	5.5	0.30	0.33	0.45
-3500	3.2	3.5	5.0	0.26	0.29	0.42
-3000	2.7	3.1	4.6	0.23	0.25	0.38
-2500	2.3	2.6	4.1	0.19	0.22	0.34
-2000	1.8	2.2	3.7	0.15	0.18	0.30
-1500	1.4	1.7	3.2	0.11	0.14	0.27
0	-	-	-	-	-	-
0	-	-	-	-	-	-
1500	1.4	1.7	3.2	0.11	0.14	0.27
2000	1.8	2.2	3.7	0.15	0.18	0.30
2500	2.3	2.6	4.1	0.19	0.22	0.34
3000	2.7	3.1	4.6	0.23	0.25	0.38
3500	3.2	3.5	5.0	0.26	0.29	0.42
4000	3.6	4.0	5.5	0.30	0.33	0.45
4500	4.1	4.5	5.9	0.34	0.37	0.49
5000	4.5	4.9	6.4	0.38	0.40	0.53

In Figure 25 are the results of the extrapolated rel. exp. MU visualised using the different extrapolation factors f_s, f_{w1}, and f_{w2}. Due to the linear increase in the scaling factor, the course of the extrapolated rel. exp MU also increasing linearly.

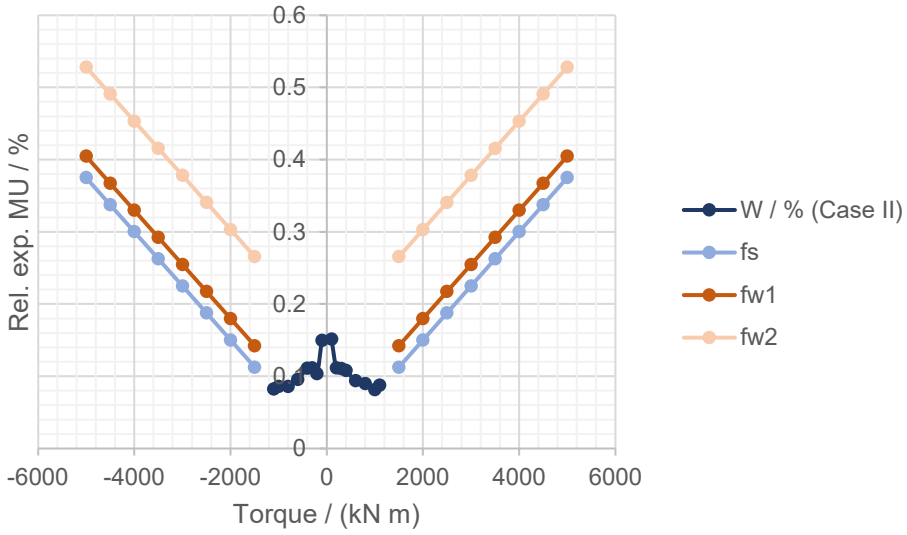

Figure 25: **Measured rel. exp. MU for the range of 100 kN m to 1.1 MN m and extrapolated rel. exp. Mus using different extrapolation factors for the range of 1.5 MN m to 5 MN m.**

The prediction factor should be selected according to different boundary conditions. These can be the later purpose of use of the transducer, additional influences such as when used under rotation and the further use and significance of the measurement results.

3.2.3 Measurement under rotation

Torque measurement up to 5 MN m under rotation up to a maximum of 20 min^{-1} can be found on the LSS of nacelle test benches (NTBs). As part of this project, the 5 MN m torque transducer was used in both a 4 MW and a 10 MW NTB at rotational speeds between 1 min^{-1} and 22.5 min^{-1}. When measuring under rotation, dynamic effects occur in the form of torque ripples. These are caused by the excitation and the general design of rotating electrical machines and the resulting change in the air gap and the non-ideal sinusoidal magnetic field. In Figure 26, the torque and rotational speed ripples with a delay of 90° measured in the 4 MW NTB of the CWD at RWTH Aachen University are depicted. The influence of the torque ripples is taken into account by averaging the torque signal under rotation over an integer number of revolutions for each load step and as a load step instability in the MU analysis of the torque measurement under rotation. [19]

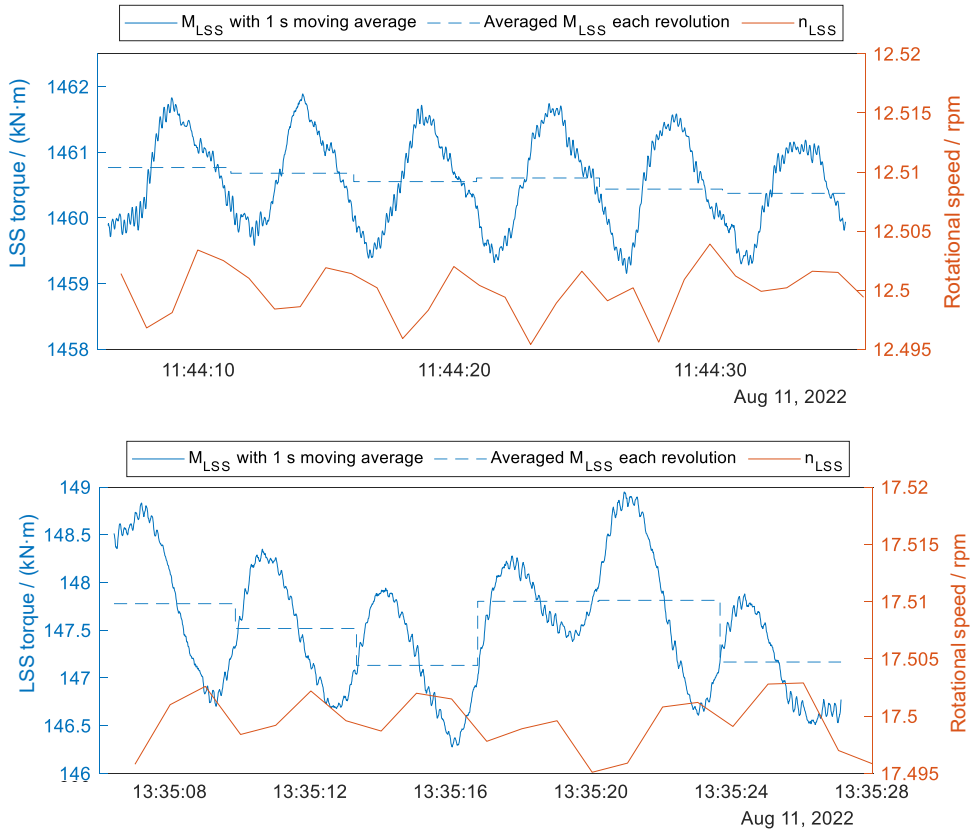

Figure 26: Torque and speed signal ripples (smoothed with a moving mean of 150 points for one second for better visualisation) over six full revolutions with a phase shift of 90° to each other at 1.5 MN m and 12.5 min^{-1}(top) and at 150 kN m at 17.5 min^{-1} (bottom) [19]**.**

From the data in Figure 26 it is evident that at higher torque steps, the variation in torque for each revolution is minimal, leading to expected periodic fluctuations in rotational speed and generator output power. Conversely, at lower torque steps, the oscillation ratio of torque increases. This reveals a more noticeable instability in the load step due to the control system: during the 5th revolution, the control system significantly increased the torque to rectify the decrease in rotational speed. Consequently, the torque exhibits a greater variation compared to higher torque steps. [19]

To assess the load step instability, the relative expanded MU $W_{M,in}$ is calculated for each load step by considering the standard deviation σ_M of the six averaged torque values:

$$W_{\mathrm{M,in}} = \frac{2\sigma_{\mathrm{M}}}{M}. \tag{30}$$

The observation in [19] reveals that within the specific speed range, the torque instability becomes more pronounced at lower torque steps.

DOI: 10.5281/zenodo.8112428

3.2.4 Calibration of the rotational speed measurement

For a traceable rotational speed measurement on an NTB, an inclinometer was developed as transfer standard to calibrate the rotary encoder used by the test bench operator.

The selected inclinometer includes two perpendicularly placed MEMS accelerometers for inclination measurement with reference to gravity. By placing the inclinometer at the centre of the drive train, the rotational speed can be determined by continuously measuring the angle position. Thanks to its stator-less measurement principle, compared to rotary encoders, it can directly be integrated in the 5 MN m torque transfer standard and mounted in front of the nacelle without any modification. This brings along a great flexibility for the mechanical transfer standard and an independence of the NTB's construction environment. [20]

The calibration of the inclinometer is explained in detail in [21]. The static calibration of the inclinometer has an expanded MU of 0.014° (k = 2) and a repeatability of 0.005°. As this transfer standard is dedicated for torque and rotational speed measurement on a LSS up to 5 MN m and 20 min^{-1} respectively, the inclinometer's range of rotational speed measurement is limited to 20 min^{-1}.

In [22], the calibrated rotational speed transfer standard was implemented on in a 10 MW NTB to establish a traceability chain of rotational speed measurement. During the evaluation of the measurement data, additional MU contributed by mounting misalignments, eccentricity, dynamic effects, and the process of data evaluation were added to the static calibration results. In the end, the inclinometer shows a rotational speed related (due to the reduced measurement time at higher rotational speed, the MU at higher speed is larger) MU as in Table 9.

Table 9: Total MU (k = 2) of the rotational speed measurement in a 10 MW NTB.

Rotational speed / min^{-1}	Absolute MU / min^{-1}	Relative MU / %
4.5	$8.1x10^{-4}$	0.018 %
5	$1x10^{-3}$	0.020 %
6	$1.4x10^{-3}$	0.024 %
7	$2x10^{-3}$	0.028 %
8	$2.6x10^{-3}$	0.032 %

To calibrate the rotary encoder used by the test bench operator, the NTB's rotary encoder was compared with the inclinometer, showing a deviation smaller than 0.009% at all measured speeds. As the deviations are smaller than the best provable MU of 0.018 % given by the inclinometer, it can be validated that the used NTB encoder can provide an equal or even lower MU than the transfer standard. Compared to the inclinometer, rotary encoders measure the rotational speed via counting pulses induced by magnetic or optic increments; their measurement accuracy is not speed related. Therefore, it is safe to conclude that the relative MU using the rotary encoder is lower than 0.02% in its entire measurement range.

4 Non-standardised torque load profiles

The most critical parameter in determining wind turbine efficiency and analysing its drive train is mechanical torque. Other than in standard torque calibration, in reality torque load due to different wind speeds is unpredictable and does not follow a given sequence. Moreover, wind gusts can cause rapid and enormous changes in torque. Hardware-in-the-Loop (HiL) tests on NTBs simulate various wind profiles, resulting in alternating and transient torque loads. Torque load in NTBs is traced to national standards via increasing and decreasing torque load cycles, but they do not meet calibration requirements to be as close as possible to the later application. In [23] two different load configurations to analyse how a transducer responds to non-traditional calibration loads are suggested. The first method, called "fast-loading profiles", applies torque under various steps and rates and measures the transducer's output reading in a shorter time than standard calibration practices. The second method, called " randomly shuffled loading profiles", takes the same torque points and measures them in a random order, with each torque point having the same stabilisation interval. These are static test methods, with zero torque rates at the time of reading. It is worth noting that digital filtering influences can be analysed in the first method under weak stabilisation conditions. These results were presented at IMEKO 24th TC3 International Conference in Cavtat-Dubrovnik, Croatia in October 2022 and are available in [23].

4.1 The 2 kN m special torque transducer

Test specimen 1 is a 2 kN m special torque transducer (Figure 27 left) manufactured by HBM (now HBK). It measures torque M_Z and force F_Z around and along the main axis z and bending moments around the x-axis M_x and the y-axis M_y. More details are listed in Table 10.

Table 10: Characteristic values of the 2 kN m special torque transducer.

Type	Value	Output signal
Nominal (rated) torque M_{nom}	2 kN m	1.2 mV/V
Torque limit, related to M_{nom}	3 kN m	-
Breaking torque, related to M_{nom}	> 300 %	-
Axial force limit	20 kN	ca. 0.2 mV/V
Shear force limit	5 kN	-
Bending moment limit	1 kN m	ca. 0.4 mV/V

For an easy and reproducible mounting, adapters with shaft ends are screwed to the transducer (Figure 27 right).

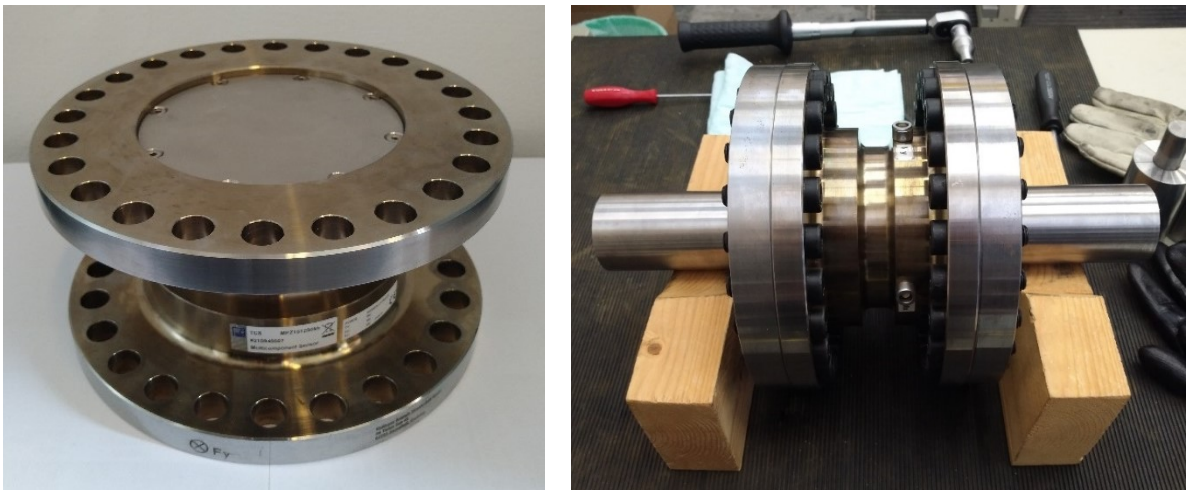

Figure 27: 2 kN m special torque transducer (M_z) with additional bridges for F_z, M_x and M_y.

4.2 The 2 kN m Raute TT2

Raute precision TT2 with a nominal torque range of 2 kN m. The transducer is a flange-type transducer that could be installed directly into the calibration device used without any adapters.

DOI: 10.5281/zenodo.8112428

4.3 Standardised torque calibration

As a reference for the further analyses, both transducers were calibrated using standard calibration procedures to evaluate their performance and deviation from the national standard in a static, step-by-step manner as described in section 2.3. The 2 kN m special torque transducer was calibrated up to 1 kN m using CMI's 1 kN m dead-weight TSM (2.2.1). The 2 kN m Raute TT2 was calibrated up to 2 kN m at VTT using their 2 kN M reference TSM (section 2.2.2). In the following, the calibration results accomplished acc. to DIN 51309 are called 'Normal'.

For all additional analyses, the measurement set-ups are the same as for DIN 51309 calibrations with the same adapters, alignment requirements, requirements on ambient conditions and stabilisation period to record the measured values, and amplifier filter settings.

4.4 Fast-loading profiles

The fast-loading profiles used here are based on Appendices A.3.1 and A.3.2 of the DKD-R 3-9 guide [24], which is intended for characterising force transducers under continuous load profiles. However, the same idea and methodologies can be applied to torque transducers to analyse the influence of fast loadings on sensitivity and hysteresis. [23]

4.4.1 Influence on the sensitivity

Here, a test for fast loading using torque applied in steps up to the nominal value is described, with measurements taken after a transient period. The test is repeated for 20 % steps up to the nominal value and digital filtering is applied at two different cut-off frequencies (0.1 Hz and 2 Hz). The measured sensitivities for each torque value are compared to the corresponding sensitivities achieved in the DIN 51309 calibration, resulting in relative differences shown in Figure 28. [23]

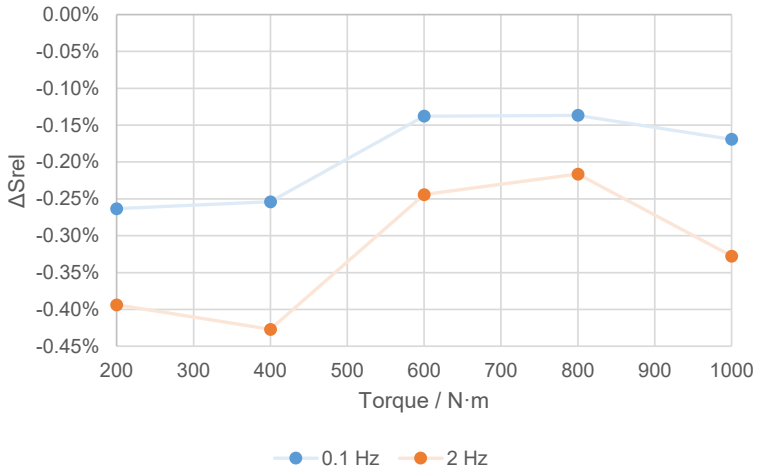

Figure 28: Relative difference between fast loading and DIN 51309 output sensitivities for different torque values and filter cut-off frequencies [23].

4.4.2 Influence on the hysteresis

The second fast loading test involves applying increasing torque from zero up to a torque point, measuring the transducer signal, returning to the starting point, and the repeating the process for other points in the range. The test also involves applying decreasing load till reaching the measuring point again and measuring the transducer signal. The hysteresis is calculated as the difference between increasing and decreasing step values, and the hysteresis for fast loadings is compared to the DIN 51309 results. The results of the test, shown in Figure 29, reveal that the torque rate and the cut-off frequency significantly affect the output sensitivity and hysteresis parameters. It is important to note that the dead-weight machine's working principles affects the hysteresis analysis due to the difference transient and oscillation responses to the incremental and decremental torque plateaus caused by the loosening of the scale pan. [23]

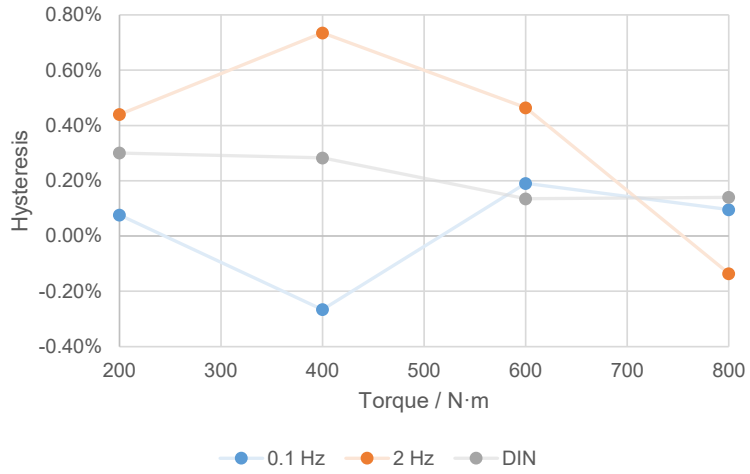

Figure 29: Hysteresis calculated for fast-loading jumps with different filter cut-off frequencies and for DIN 51309 [23]**.**

4.5 Randomly shuffled loading profiles

To examine how changes in the calibration load cycle affect the use of a previous DIN 51309 metrological characterisation, a randomised load cycle was created. The points measured were the same as in the standard method, but their order of application was shuffled in the cycle (Figure 30). The same shuffled load cycle was used for all three mounting positions to ensure a sole analysis of the randomised effect. [23]

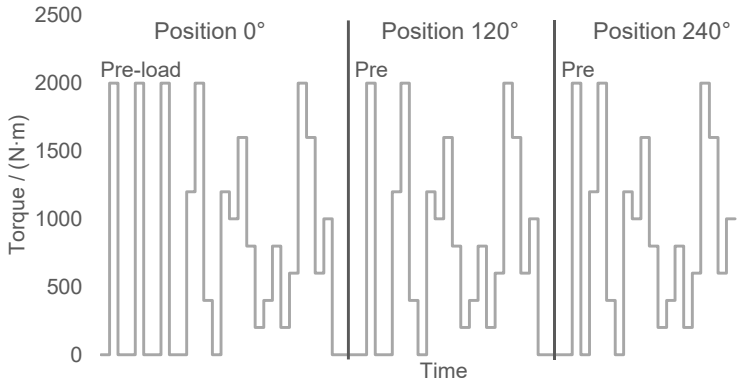

Figure 30: Randomly shuffled load points within one load cycle, repeated in different mounting positions [23]**.**

The measurement set-up was the same as for DIN 51309 calibrations. First, a complete calibration according to DIN 51309 was carried out, and the results (called 'Normal') served as reference to compare with the randomised loads. The deviations between the average measurements of ‘Normal’ and ‘S-Random’ were calculated, and the transducer output sensitivity per torque step was also evaluated. The output sensitivities for ‘Normal’ and ‘S-Random’ (randomly shuffled values were sorted: previous value lower than actual value, actual value is denoted as decreasing value) were calculated using the same reference torque vector, while for the ‘U-Random’, the output sensitivities were calculated using the transducer output intervals and the reference torque intervals occurring at the time of the reading. [23]

Figure 31 illustrates a comparison between the linearity deviation curves for 'Normal' and 'S-Random'. It is evident that 'S-Random' struggles to match the linearity path of 'Normal', despite remaining within the deviation limits. [23]

DOI: 10.5281/zenodo.8112428

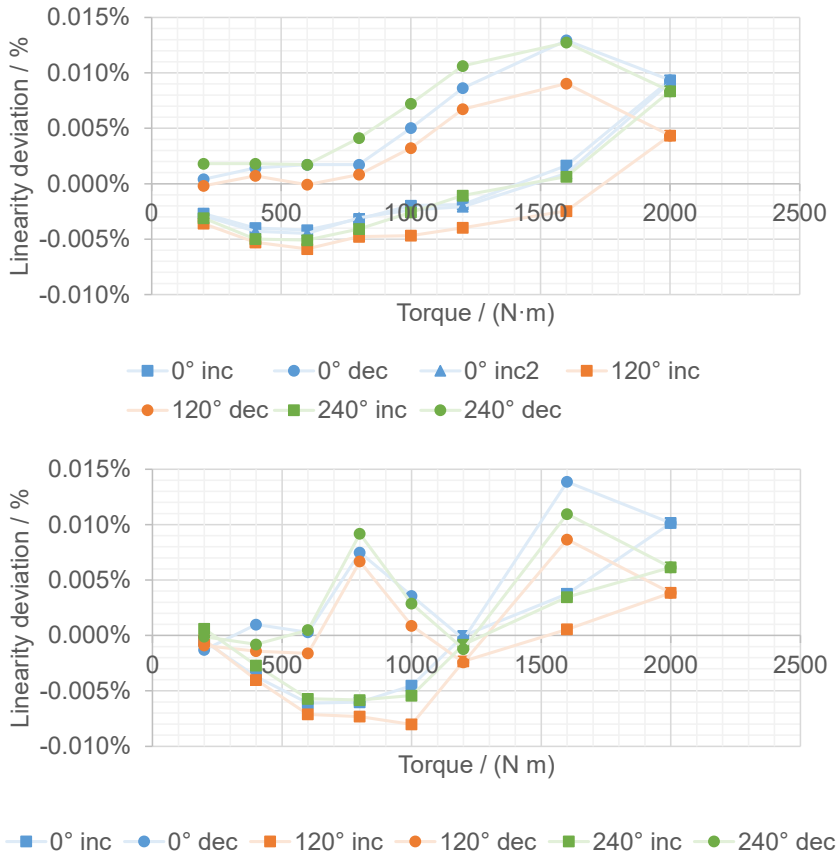

Figure 31: Linearity analysis for 'Normal' (top) and 'S-Random' (bottom) load profiles [23].

When calculating the MU using DIN 51309, the behaviour depicted in Figure 32 may be observed. The uncertainty for the cubic interpolation method is constrained only by the uncertainty of the reference torque values. However, the linear curve regression method displays considerably higher values. It is noticeable that for the 'Normal' data (in grey), there is a trend of decreasing MU as the torque increases. In contrast, for the 'S-Random' data (in yellow), this tendency is not as apparent, especially in the beginning and middle of the torque range. [23]

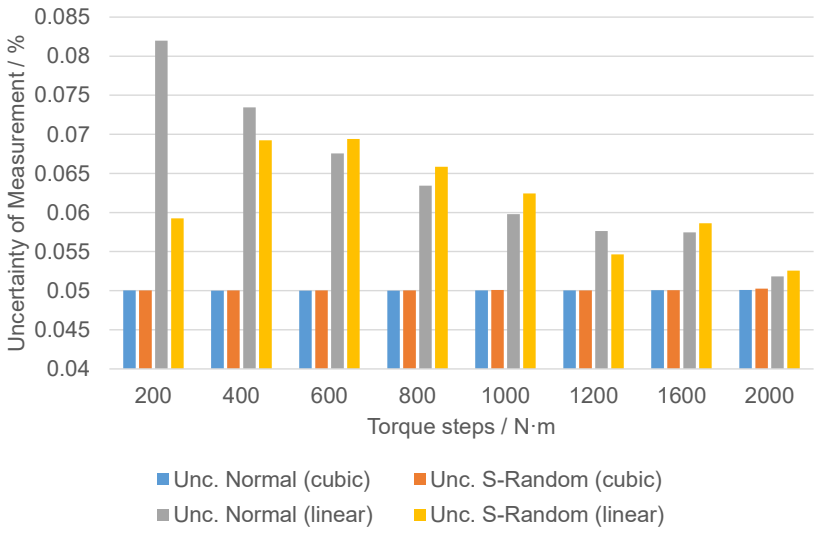

Figure 32: Expanded measurement uncertainties (k = 2) for 'Normal' and 'S-Random' data [23].

It can be summarised that torque values measured under non-traditional or non-standard conditions reveal how transducers are affected by different conditions and load profiles. Factors like previous load, creep, and hysteresis influence the measurements, even though the measurement plateaus remain stable over time. Signal processing is crucial for accurately interpreting the observed phenomenon. Further research is necessary to explore signal processing, particularly for transient and oscillatory conditions. [23]

The proposed tests involve load characteristics that deviate from traditional calibration procedures but are still within the static regime. The findings suggest that analysing the responses of torque transducers under non-static regimes, such as the load profiles used in NTBs, requires further investigation. Future research should focus on continuous and dynamic load regimes, which have non-stable plateaus and higher torque rates. [23]

DOI: 10.5281/zenodo.8112428

5 Applicability of calibrated torque transducers under rotation

As elaborated in the previous chapters, the conditions for application of torque transducers are remarkably different from the static calibration. Besides the rapid changes of loads with randomised sequence that described in chapter 4, the influence of rotation and the change of measurement chain should be considered as well.

In the static torque calibration, for each step, the load is kept constant and stable which is ideal. The remaining noise in the output is further reduced by the data acquisition (DAQ) system with a lowpass filter. A 0.2 Hz Bessel lowpass filter is commonly used at PTB for most torque calibrations.

On the drive train test bench, however, rotary torque is coupled with unneglectable ripples and oscillations. Also, the processing of torque signals is different as in the calibration. On test benches for electrical machines, power analysers are commonly to measure electrical and mechanical power simultaneously. These power analysers process both electrical and mechanical quantities during the same time interval, allowing for continuous online efficiency calculation. To suppress noise and oscillation, power analysers calculate the average torque value within this time interval. Therefore, the mathematical process used by a power analyser is also different from the lowpass filter utilised in calibration procedure.

Therefore, the applicability of the calibration results should be determined before transferring them directly to the test bench application. This chapter aims to examine the problematic by connecting two torque measurement chains in parallel during calibration measurement and test bench measurement. [25]

5.1 The T10F / T12HP torque transducers

For torque measurement under rotation, two transducers manufactured by HBK equipped with telemetric data transfer and power supply are used. T12HP is with a nominal torque of 2 kN m and a nominal rotational speed of 12000 min^{-1}. As a high-precision transducer, T12HP is integrated in the test bench drive train by connected in series with the available 3 kN m T10F (Figure 33). The technical details of the two transducers can be found in Table 11.

Figure 33: T10F 3 kN m torque transducer (left) and T12HP 2 kN m torque transducer (right) used for rotary torque measurement [www.hbm.com].

Table 11: Characteristic values of T12HP and T10F torque transducers.

Model		T12HP	T10F
Nominal torque		2 kN m	3 kN m
Frequency output (Datasheet)	Counter-clockwise nominal	90 kHz	15 kHz
	Zero	60 kHz	10 kHz
	Clockwise nominal	30 kHz	5 kHz
Calibrated sensitivity (Case II clockwise and anti-clockwise torque)		66.6660 N m / kHz	599.392 N m / kHz
Calibrated accuracy class 200 N m to 2000 N m (classes 0.05 to 5 acc. to DIN 51309)		0.05	0.2

5.2 Static torque calibration

In order to have a direct comparison between the torque values measured by the power analyser and those measured during the calibration, the T12HP and T10F torque transducers were installed on the beforementioned 20 kN m TSM to perform a static torque calibration according to DIN 51309 (Figure 34). As T12HP is more accurate compared to T10F, the signals of T12HP are evaluated for analysis.

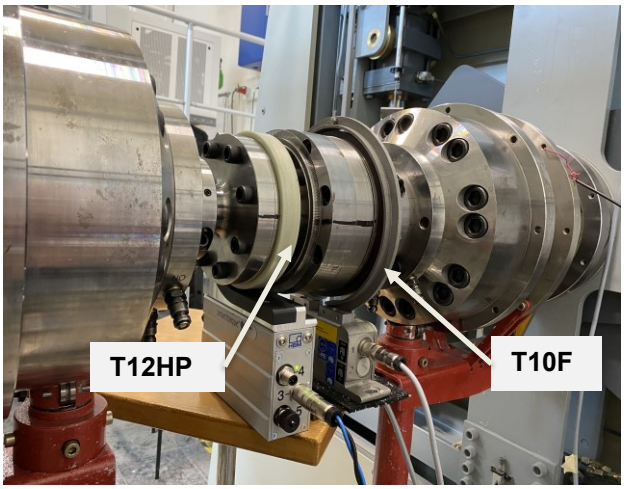

Figure 34: Static calibration of the T12HP and T10F torque transducers in the 20 kN m TSM at PTB.

As illustrated in Figure 35, T12HP is loaded by defined torque steps by the TSM and produces a frequency impulse output that is utilized to feed both measurement chains in parallel for analysis. The MGCplus DAQ system, together with an ML60B measurement card, reads the output signal using a 0.2 Hz Bessel lowpass filter at a 10 Hz sampling rate. For every load step, a single measurement value is compared to the defined torque load for calibration purposes. This technique is referred to as "LP" in the subsequent discussions. [25]

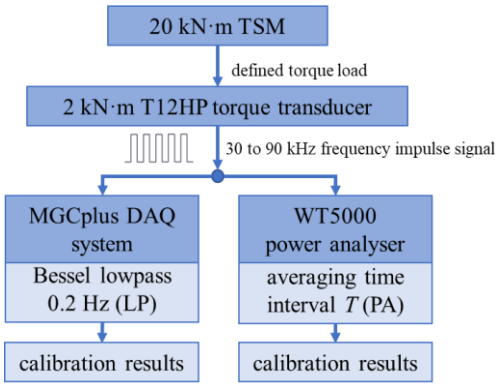

Figure 35: Calibration setup for the T12HP torque transducer according to DIN 51309 with additional power analyser measurement [25].

Furthermore, the transducer's output signal is simultaneously fed into the Yokogawa WT5000 power analyser, in addition to the so-called traditional measurement chain, allowing for calibration of this measurement chain used in motor test bench as well. The power analyser processes the transducer's frequency signal at a megahertz sampling frequency range and records the average value continuously over a specified time interval *T*. This method is referred to as "PA" in the subsequent discussions. For both measurement chains, the torque signal is recorded after a 33 s dwelling time in each load step. [25]

DOI: 10.5281/zenodo.8112428

Figure 36 is presented for the calibration results obtained using different recording methods according to DIN 51309. Each curve in the presented figures indicates the linearity deviation of the transducer's output signal with respect to the maximum calibrated torque for both increasing and decreasing load steps (inc and dec). The torque is measured in both clockwise (quadrants I and IV) and anticlockwise (quadrants II and III) directions for three different mounting positions (0°, 120°, and 240°). [25]

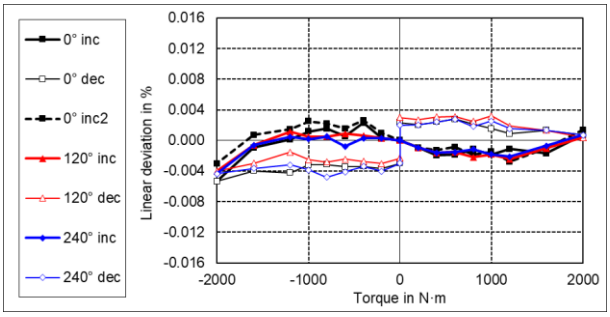

(a) Rel. linearity deviation with LP (using MGCplus and 0.2 Hz Bessel lowpass filter)

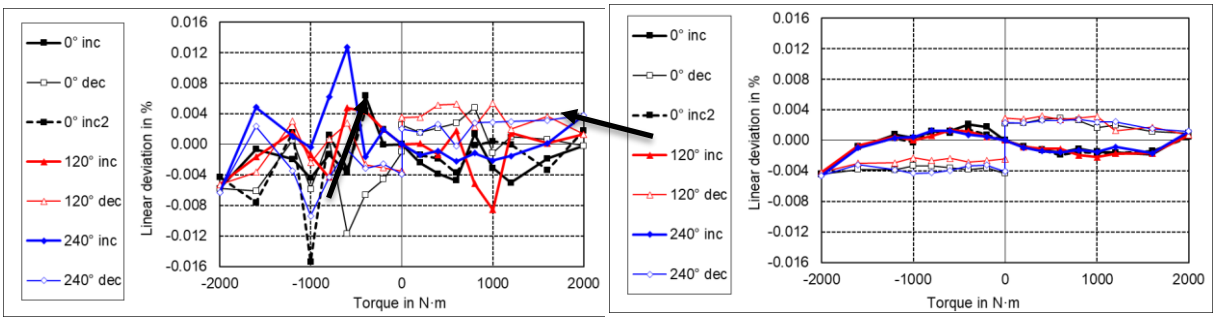

(b) Rel. linearity deviation with PA (using power analyser T = 1 s)

(c) Rel. linearity deviation with PA (using power analyser T = 8 s)

Figure 36: Comparison of the torque calibration results using the different recording methods [25]**.**

Figure 36 (b) illustrates the torque deviation measured by the power analyser with an averaging time of one second (T = 1 s). The figure indicates that the torque is measured with noticeably higher and randomly distributed deviations. This implies that the one second averaging time is insufficient to reduce noise and oscillation to the same extent as the 0.2 Hz Bessel filter. However, Figure 36 (c) shows that with an averaging time of eight seconds (T = 8 s), the torque can be measured with an accuracy that is comparable to that of the static calibration. [25]

5.3 Usage under rotation

Expanding the comparison of the two measurement chains from static to dynamic conditions, the torque transducer that has been statically calibrated is mounted on a 200 kW electrical machine test bench at PTB, as depicted in the Figure 37. A universal joint connects the specimen on the left to the DC load motor on the right, with the calibrated transducer positioned between them to measure the torque. Additionally, the transducer is equipped with an optical incremental encoder that allows for the measurement of rotational speed during testing. [25]

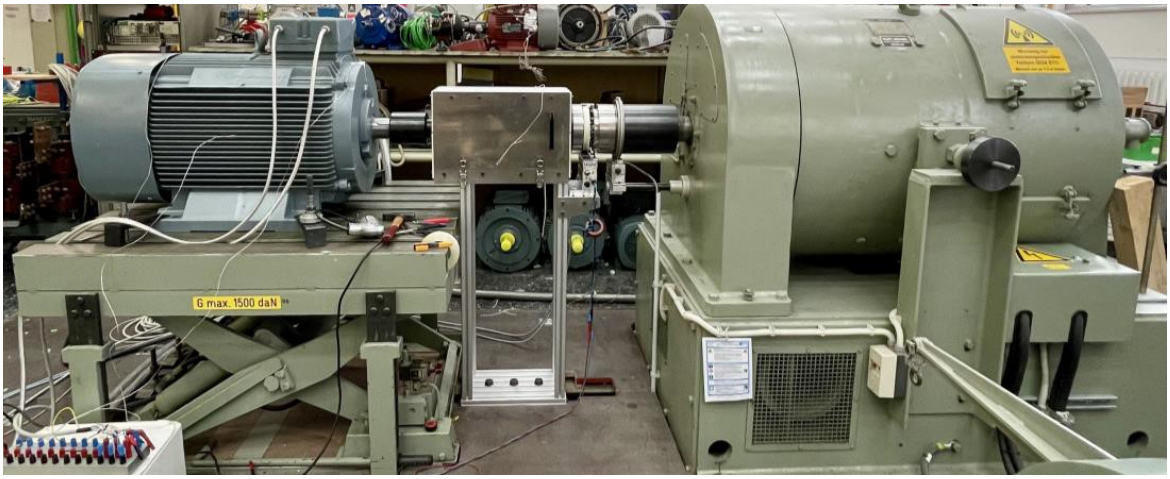

Figure 37: **The 200 kW test bench with a specimen on the left and a DC load motor on the right as well as the torque transducer in between** [25]**.**

The measurement chains as in the Figure 35 is replicated on the test bench, except for the MGCplus being substituted with a QuantumX MX460b. This alternative equipment operates on the same measurement principles and offers similar levels of accuracy. To enhance the clarity of the process within the power analyser, a half-second averaging time interval (T = 0.5 s) is selected, and the averaged data are subsequently subjected to a 16-point moving average filter. As a result, the measurement chain is equivalent to the T = 8 s setting presented in Figure 36 (c). [25]

Throughout the measurement process, a characterisation map is generated to explore the correlation between the measured torque and the rotational speed over a wider range of specimen operation. Figure 38 illustrates the measured rotational speed and raw torque data, alongside the lowpass filtered signal (LP) and the averaged signal obtained through the power analyser (PA). [25]

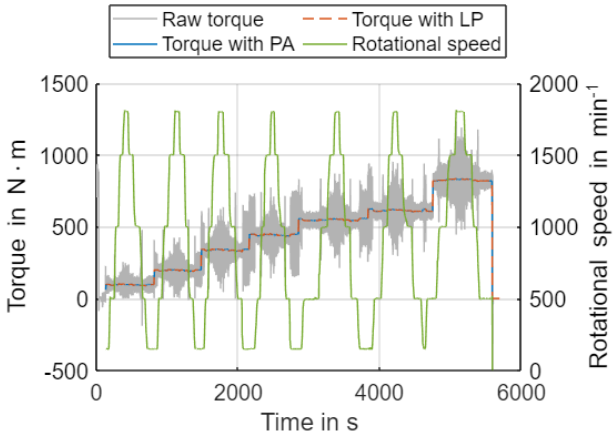

Figure 38: **Performed characterisation map consisting of measured torque and rotational speed** [25]**.**

5.3.1 Measurement point stability

Figure 38 shows that the torque measurements on the test bench exhibit significant oscillations or torque ripples, especially at the upper and lower speed limits. Two load steps are selected to investigate how LP and PA behave under torque ripples. [25]

- Case A: load step at 830 N m and 1000 min^{-1}

The complete course of the load step is presented in Figure 39 (a). In Figure 39 (b), the time axis is enlarged in (zoom area (b)), and in Figure 39 (c), the torque axis is enlarged in (zoom area (c)).

DOI: 10.5281/zenodo.8112428

Since the amplitude ratio of the torque ripples is relatively small at this load step compared to other steps, both LP and PA methods are able to effectively reduce the torque ripples and provide stable measurements. [25]

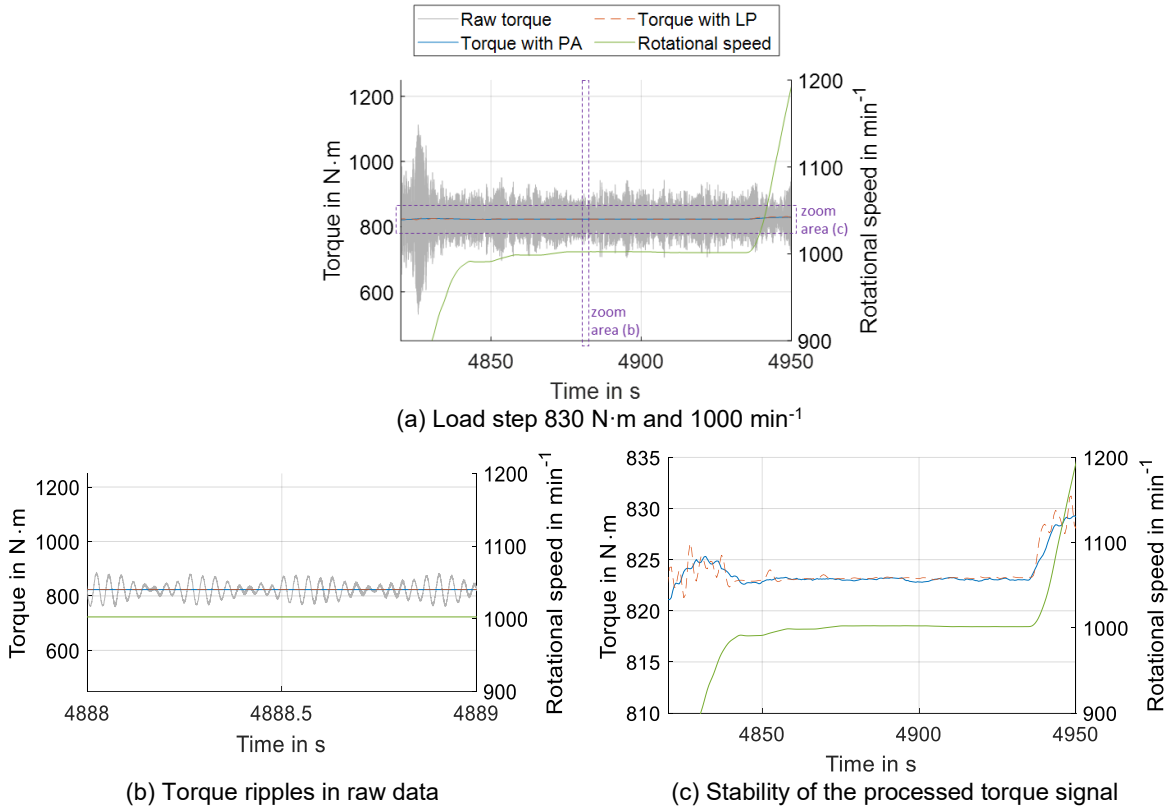

(a) Load step 830 N·m and 1000 min^{-1}

(b) Torque ripples in raw data

(c) Stability of the processed torque signal

Figure 39: Stability of the torque measurement at load step 830 N m and 1000 min^{-1} [25]**.**

- Case B: load step 830 N m and 1800 min^{-1}

The complete course of the load step is presented in Figure 40 (a). In Figure 40 (b), it is enlarged in on the time axis (zoom area (b)), while in Figure 40 (c), a zoom is shown on the torque axis (zoom area (c)).

Compared to other load steps, the amplitude ratio of the torque ripples is much larger at this particular load step. In this case, LP achieves better stability, while the processed signal of PA shows an up-and-down movement. This is partly due to the fact that the averaging method of PA is not capable of reducing the ripples to the same level as LP. Furthermore, the torque ripples pose a challenge to the control system to maintain a constant load step, as evidenced by the fact that the mean values of both torque and speed continue to change even after dwell. [25]

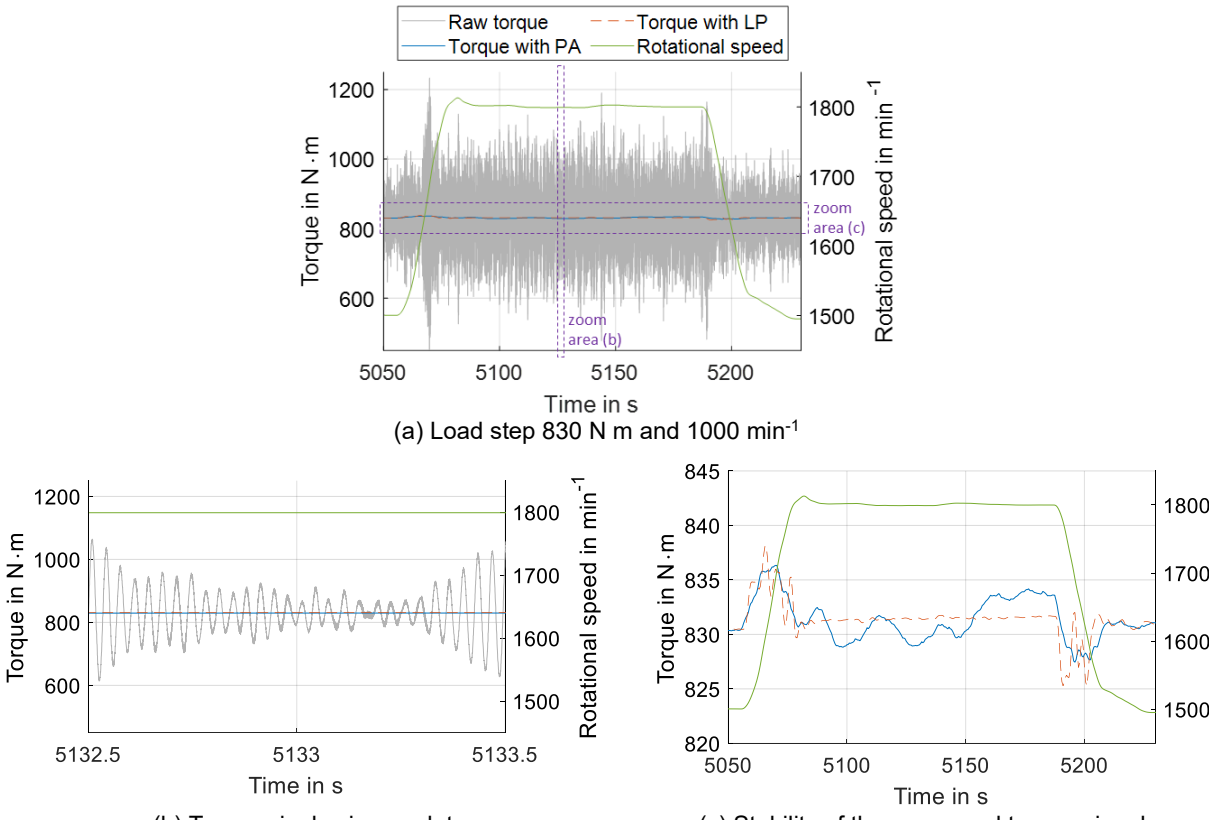

(a) Load step 830 N m and 1000 min^{-1}

(b) Torque ripples in raw data

(c) Stability of the processed torque signal

Figure 40: Stability of the torque measurement at load step 830 N m and 1800 min^{-1} [25]**.**

5.3.2 Uncertainty contribution due to instability

The corrected relative standard deviation for each load step, with LP and PA, is presented in the characterisation matrix shown in Figure 41.

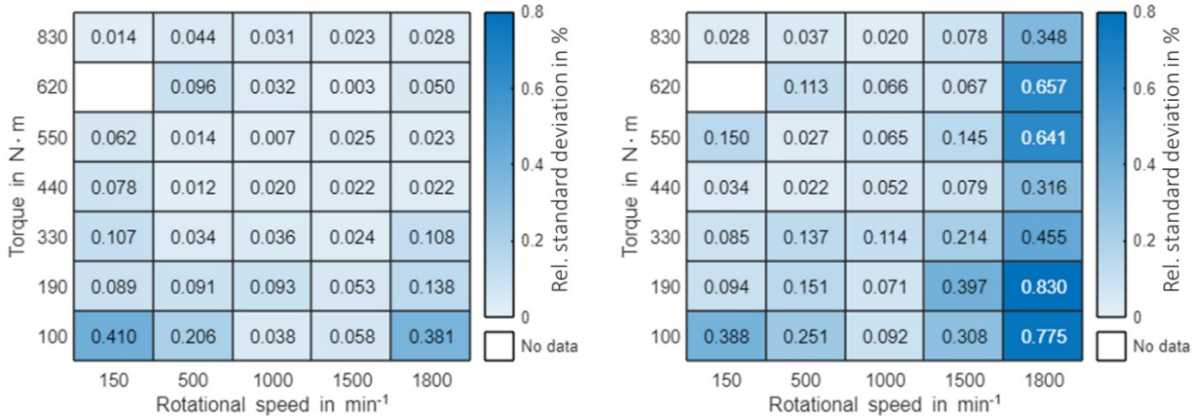

(a) Corrected relative standard deviation with LP in %

(b) Corrected relative standard deviation with PA in %

Figure 41: Characterisation matrix of the corrected relative standard deviation with LP or PA for each load step ("No data" means that the load step is too short for analysis) [25]**.**

In summary, it is important to take into account the torque instability as an additional source of uncertainty when measuring torque on a test bench, as the instability of load steps can significantly impact measurement accuracy. This effect becomes particularly pronounced in the presence of severe torque ripples, emphasizing the need for careful consideration and calibration of measurement equipment in such scenarios. [25]

DOI: 10.5281/zenodo.8112428

6 Summary and recommendations

There are currently no ways to calibrate torque under rotation – especially not in the meganewton-metre range, which is required for test in the wind energy sector. To make matters worse, even a static torque calibration above 1.1 MN m is still not possible. Nevertheless, in order to enable a partially traceable torque measurement in the meganewton-metre range under rotation in test benches for wind turbine drive trains, this report describes the partial range calibration of a 5 MN m transfer standard up to 1.1 MN m, further characterisations for establishing a transfer standard, three extrapolation options for the calibration result, and one in-depth analysis for torque measurement under rotation up to 22.5 min^{-1} performed with the transfer standard. With a rel. exp. MU of 0.08 % (k = 2), the partial range calibration of the 5 MN m transfer standard is below the required target of < 0.1 %. However, the influence of rotation has not yet been considered here. Values between 0.29 % and 0.65 % [19] were determined as the real overall rel. exp. MU for the torque measurement under rotation in a test bench, taking into account the dynamic effects (4 MW NTB with translating 2.75 MW DUT with full converter).

A 125 kN m torque transducer was calibrated statically up to 125 kN m with a rel. exp. MU of 0.08 % (k = 2) for measurements on the HSS of a wind turbine drive train. Moreover, the usage of statically calibrated torque transducers under rotation was investigated on a small-scale electric motor test bench. When using a power analyser with a short averaging time, it must be noted that the accuracy of the torque transducer is significantly lower than that specified in the calibration certificate. To avoid this, the averaging time should be adjusted according to the lowpass filter for the static calibration. In [24], it is recommended to use an averaging time of at least 8 s for torque and rotational speed measurement on the HSS to ensure a minimum measurement quality. Other than on the LSS, the averaging interval does not need to be an integer number of shaft revolutions. When combining the measurements on the HSS with measurements on the LSS, however, the same averaging interval should be used, the length of which is determined by the integer rotations of the LSS.

Since both real wind loads and simulated wind loads in test benches are not strictly increasing or decreasing, the influence of non-traditional calibration load sequences on the torque measurement was also investigated. It turned out that both the influence of the previous load and the creep and hysteresis phenomena have an influence and that the method and the parameters adopted during signal processing have an enormous contribution to the correct interpretation of the measured phenomenon.

DOI: 10.5281/zenodo.8112428

I Bibliography

[1] R. Schicker und G. Wegener, Measuring Torque Correctly, Bielefeld: Bentrup Druckdienste KG, 2002.

[2] K. Hoffmann, „An introduction to stress analysis and transducer design using strain gauges“.

[3] *ISO 376:2011 Metallic materials — Calibration of force-proving instruments used for the verification of uniaxial testing machines,* International Organization for Standardization, 2011-06.

[4] J. Fidelus, J. Puchalski, A. Trych-Wildner und P. Weidinger, „The creep behaviour of a 2 kN m torque transducer tested at GUM and PTB,“ in *MEASUREMENT 2023, Proceedings of the 14th International Conference*, Smolencie, Slovakia, 2023.

[5] P. Weidinger, G. Foyer, J. Ala-Hiiro, C. Schlegel und R. Kumme, „Investigations towards extrapolation approaches for torque transducer characteristics,“ *J. Phys.: Conf. Ser. 1065 042057,* 2018.

[6] D. Peschel, D. Mauersberger, D. Schwind und U. Kolwinski, „The new 1.1 MN m torque standard machine of the PTB Braunschweig / Germany,“ in *Conference on Force, Mass and Torque, 19th IMEKO TC3*, Cairo, Egypt, 2005.

[7] H. Kahmann, K. Geva, C. Schlegel, R. Kumme und F. Härtig, „Final design of PTB's 5 MN m torque standard machine with possible future extension to 20 MN m,“ in *IMEKO 24th TC3, 14th TC5, 6th TC16 and 5 th TC22 International Conference*, Cavtat-Dubrovnik, Croatia, 2022.

[8] *EURAMET cg-14: Guidelines on the Calibration of Static Torque Measuring Devices,* EURAMET e.V., 2011.

[9] *DIN 51309: 2013-09 Material testing machines - calibration of static torque measuring devices,* Berlin: DIN Deutsches Institut für Normung e.V., 2013.

[10] J. Michalec, Mechanics of material II, part 3.2 Rotating discs, Czech technical university Prague.

[11] „HiL-GridCoP,“ Fraunhofer IWES, [Online]. Available: https://www.iwes.fraunhofer.de/en/research-projects/finished-projects-2022/hil-gridcop.html. [Zugriff am 06 02 2023].

[12] *T40FH: Genauer Drehmomentmessflansch zum Messen hoher Drehmomente.*

[13] *Remarks to calibrations and calibration certificates,* 2023.

[14] *Evaluation of measurement data - Guide to the expression of uncertainty in measurement,* JCGM, 100:2008.

[15] J. D. Fidelus, J. Puchalski, A. Trych-Wildner, M. Urbaski und P. Weidinger, „Torque transducer uncertainty estimation in the MN m range - classical approach and fuzzy sets,“ *MDPI Energies,* Bd. Submitted, 2023.

[16] *Calibration Certificate up to 1.1 MN m issued by PTB,* serial no.: 193840001, 08.01.2021.

[17] *Report on extrapolation of high forces and the associated uncertainty,* EMRP-Project "Force Traceability within the meganewton range".

[18] Z. Song, P. Weidinger, M. Zweiffel, A. Dubowik, C. Mester, N. Yogal und R. S. Oliveira, „Traceable efficiency determination of a 2.75 MW nacelle on a test bench,“ *Engineering Research by Springer,* Bd. in preparation, 2023.

[19] Zihang Song, Paula Weidinger, Norbert Eich, Hongkun Zhang, Nijan Yogal, Rolf Kumme, „10 MW MECHANICAL POWER TRANSFER STANDARD FOR NACELLE TEST BENCHES USING A TORQUE TRANSDUCER AND AN INCLINOMETER,“ in *XXIII IMEKO World Congress “Measurement: sparking tomorrow’s smart revolution”*, Yokohama, 2021.

[20] Z. Song, P. Weidinger, L. Vavrečka, M. Heller, J. Fidelus, R. S. de Oliveira, M. Zweiffel und T. Kananen, „Deliverable D2 wihtin the EMPIR WindEFCY project No. 19ENG08: Report describing the requirements of tachometers such as the evaluation of existing tachometer measuring principles and their capabilities, and the procedure developed to calibrate...,“ 2021.

DOI: 10.5281/zenodo.8112428

[21] Zihang Song, Paula Weidinger, Hongkun Zhang, Marcel. Heller, Rafael Soares Oliveira and Rolf Kumme, „Metrological characterisation of rotational speed measurement using an inclinometer in a nacelle test bench," in *Sensoren und Messsysteme 2022*, Nürnberg, 2022.

[22] R. S. Oliveira, P. Weidinger, Z. Song, L. Vavrečka, J. Fidelus, T. Kananen und S. Kilponen, „Transducer response under non-standardised torque load profiles," in *IMEKO 24th TC3, 14th TC5, 6th TC16 and 5 th TC22 International Conference*, Cavtat-Dubrovnik, Croatia, 2022.

[23] *Richtlinie DKD-R 3-9: Kontinuierliche Kalibrierung von Kraftaufnehmern nach dem Vergleichsverfahren,* Braunschweig, Germany: Physikalisch-Technische Bundesanstalt, 09/2018.

[24] Z. Song, P. Weidinger, N. Yogal, R. S. de Oliveira, C. Lehrmann und R. Kumme, „Applicability of torque calibration on test benches for electrical machines," in *IMEKO 24th TC3, 14th TC5, 6th TC16 and 5th TC22 International Conference*, Cavtat-Dubrovnik, 2022.

[25] P. Weidinger, Z. Song, R. S. d. Oliveira, N. Yogal, A. Dubowik, C. Lehrmann, C. Mester, M. Heller, H. Zhang, M. Zweiffel, J. M. Quintanilla Crespo, C. Sarobe Carricas und J. Hällström, „Summary report describing the schedules for the three measurement campaigns to determine the efficiency of nacelles and their components on test benches with a target uncertainty of 1 % including pre-tests, measuring devices, and transfer standard spec...," zenodo.org, 2022.

II Acronyms

CM	calibration machine
CMI	Czech Metrology Institute
CWD	Center for Wind Power Drives
DAQ	data acquisition
DC	direct current
DIN	Deutsches Institut für Normung
DUT	device under test
DyNaLab	dynamic nacelle testing laboratory
EMPIR	European Metrology Programme for Innovation and Research
EU	European Union
FhG IWES	Fraunhofer Gesellschaft - Institut für Windenergiesysteme
GUM	Central Office of Measures
HBK	Hottinger, Brüel & Kjær
HiL	Hardware-in-the-Loop
HiL-GridCoP	
HSS	high-speed shaft
Inmetro	National Institute of Metrology, Quality and Technology
LP	lowpass filtered signal
LPU	law of propagation of uncertainty
LSS	low-speed shaft
MCM	Monte Carlo Method
MU	measurement uncertainty
NMI	national metrology institute
NTB	nacelle system test bench
PA	power analyser
PTB	Physikalisch-Technische Bundesanstalt
RWTH	Rheinisch-Westfälische Technische Hochschule Aachen
SG	strain gauge
TSM	torque standard machine
VTT	Technical Research Centre of Finland Ltd.
WindEFCY	Wind efficiency
WLS	weighted least squares method
WP2	Work Package 2

DOI: 10.5281/zenodo.8112428

III Acknowledgements

The project 19ENG08 – WindEFCY has received funding from the EMPIR programme co-financed by the Participating States and from the European Union's Horizon 2020 research and innovation programme.